

Synthesis and Characterization of Amine Intercalated Ca-Bentonite

by

Muhammed Azhar Bin Abdul Alim Sidique

Dissertation submitted in partial fulfillment of
the requirements for the
Bachelor of Engineering (Hons)
(Chemical Engineering)

DECEMBER 2009

Universiti Teknologi PETRONAS
Bandar Seri Iskandar
31750 Tronoh
Perak Darul Ridzuan

CERTIFICATION OF APPROVAL

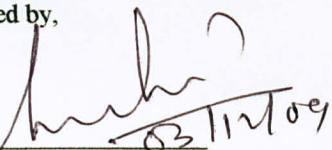
Synthesis and Characterization of Amine Intercalated Ca-Bentonite

by

Muhammed Azhar B Abdul Alim Sidique

**A project dissertation submitted to the
Chemical Engineering Programme
Universiti Teknologi PETRONAS
in partial fulfilment of the requirement for the
BACHELOR OF ENGINEERING (Hons)
(CHEMICAL ENGINEERING)**

Approved by,


(AP. Dr. Saikat Maitra)

Assoc. Prof Dr Saikat Maitra
Associate Professor
Chemical Engineering Department
Universiti Teknologi PETRONAS

UNIVERSITI TEKNOLOGI PETRONAS

TRONOH, PERAK

November 2009

CERTIFICATION OF ORIGINALITY

This is to certify that I am responsible for the work submitted in this project, that the original work is my own except as specified in the references and acknowledgements, and that the original work contained herein have not been undertaken or done by unspecified sources or persons.



MUHAMED AZHAR BIN ABDUL ALIM SIDIQUE

ABSTRACT

This report basically discusses the research done and basic understanding of the chosen topic, which is Syntheses and Characterization of Amine Intercalated Ca-Bentonite. The objective of the project is to develop clay which has been intercalated with various types of amine solvents. Research was done to develop clays intercalated with suitable molecules and surface treated as well as to study the characterization of the intercalated materials. This report will further discuss on the structure and the composition of the clay mineral, besides indulging deeper on the physical and chemical properties of Bentonite clay, or commonly known as Smectites. This report will also further discuss on types of amines and their physical properties. Next, the report will discuss on the experimental procedures involved in this project. The results from the experiment will be discussed in the end of this report which basically covers the characterization processes on different types of intercalated and pure bentonite clays.

ACKNOWLEDGEMENTS

I would like to express my gratitude to all those who gave me the possibility to complete this exploratory final year research project. First of all, I want to thank to Chemical Engineering Department and Mechanical Engineering Department of Universiti Teknologi Petronas, for giving me permission to commence this exploratory final year project in the first instance, to do the necessary research work and to use the facilities under their department purview.

I am deeply indebted to my supervisor Associate Professor Dr. Saikat Maitra from Chemical Engineering Department whose supportive help, stimulating suggestions and encouragement helped me in all the time of research for and writing of this thesis. Also, I would like to express my gratitude to the lab technicians and my fellow research mate, Mr. Ali Eltayeb for all the guidance and assistance throughout completing this project.

Also, special thanks to my family whose advice, love and support enabled me to complete this work. The completion of this document would not have been possible without the support, hard work and endless efforts of a large number of individuals and institutions.

TABLE OF CONTENTS

ABSTRACT.....	iii
ACKNOWLEDGEMENTS.....	iv
CHAPTER 1	1
1.1 Background.....	1
1.2 Problem Statement	1
1.3 Objectives and Scope of Study.....	2
CHAPTER 2	3
2.1 Clays and Clay Minerals	3
2.1.1 Structure and Compositions of Clay Mineral.....	3
2.1.2 Chemical and Physical Properties of Smectite Clays.....	5
2.1.3 Intercalation Behaviour of Montmorillonite into Layered Silicates in Organic Solvents	6
2.2 Comparison of Amine Solutions	6
2.2.1 Monoethanolamine, MEA.....	7
2.2.2 Diethanolamine, DEA	7
2.2.3 Diglycolamine, DGA	8
2.2.4 Methyldiethanolamine, MDEA.....	8
2.4 Cation Exchange Capacity (CEC).....	14
CHAPTER 3	15
3.1 Experimental Procedures	15
CHAPTER 4	17
4.1 Synthesis of Amine-Intercalated Ca-Bentonite	17
4.2 Characterization of Amine-Intercalated Ca-Bentonite	19
4.2.1 Fourier Transform Infrared Spectroscopy (FTIR).....	19
4.2.2 X-ray Diffraction (XRD).....	19
4.2.3 Scanning Electro Microscopy (SEM).....	28
4.2.4 Thermogravimetric Analysis (TGA).....	19
CHAPTER 5	47
5.1 Conclusion	17
REFERENCES.....	46
APPENDIX	

LIST OF FIGURES

Figure 1: Diagrammatic Sketch of Octahedral Sheet	4
Figure 2: Diagrammatic Sketch of Tetrahedral Sheet	4
Figure 3: General Molecular Structure of Amines	6
Figure 4: Primary amines.....	6
Figure 5: Secondary amines.....	7
Figure 6: Tertiary amines.....	7
Figure 7: Molecular structure of DEA.....	7
Figure 8: Molecular structure of MDEA	8
Figure 9: Arrangement of SEM	11
Figure 10: Overall FTIR Process.....	14
Figure 11: Stirring Process of the clay slurry	15
Figure 12: The results from the centrifuge process	12
Figure 13: The supernatant layers collected in a beaker for sodium testing	13
Figure 14: The dried Bentonite Clay	18
Figure 15: Prepared intercalated samples	19
Figure 16: FTIR Graph for Pure Bentonite.....	21
Figure 17: FTIR Graph for Ca-Bentonite	21
Figure 18: FTIR Graph for EA-Ca-Bentonite	22
Figure 19: FTIR Graph for DEA-Ca-Bentonite.....	22
Figure 20: FTIR Graph for TEA-Ca-Bentonite	23
Figure 21: XRD image for Pure Bentonite	24
Figure 22: XRD image for Ca-Bentonite.....	24
Figure 23: XRD image for EA-Ca- Bentonite	25
Figure 24: XRD image for DEA-Ca-Bentonite	25
Figure 25: XRD image for TEA-Ca-Bentonite	26
Figure 26: SEM Image: Pure Bentonite & Ca-Bentonite with 100 Magnification	27
Figure 27: SEM Image : Pure Bentonite and Ca-Bentonite with 5k Magnification.....	27
Figure 28: SEM Image:Pure Bentonite and EA-Ca-Bentonite 5k Magnification	27
Figure 29: SEM Image: Pure Bentonite and EA- Ca-Bentonite 100 Magnification	28
Figure 30: SEM Image: Pure Bentonite and DEA- Ca-Bentonite 100 Magnification ...	28

Figure 31: SEM Image: Pure Bentonite and DEA- Ca-Bentonite 5k Magnification 28

Figure 32: SEM Image: Pure Bentonite and TEA- Ca-Bentonite 100 Magnification.... 29

Figure 33: SEM Image: Pure Bentonite and TEA- Ca-Bentonite 100 Magnification.... 29

Figure 34: Graph of weight(%) vs. Temperature for Pure Bentonite 31

Figure 35: Graph of weight(mg) vs. Temperature for Pure Bentonite 31

Figure 36: Graph of derivative weight (%/min) for Pure Bentonite..... 32

Figure 37: Graph of weight(%) vs. Temperature for Ca-Bentonite..... 34

Figure 38: Graph of weight(mg) vs. Temperature for Ca-Bentonite..... 34

Figure 39: Graph of derivative weight (%/min) for Ca-Bentonite 35

Figure 40: Graph of weight(%) vs. Temperature for EA-Ca-Bentonite 37

Figure 41: Graph of weight(mg) vs. Temperature for EA-Ca-Bentonite 37

Figure 42: Graph of derivative weight (%/min) for EA-Ca-Bentonite..... 38

Figure 43: Graph of weight(%) vs. Temperature for DEA-Ca-Bentonite 40

Figure 44: Graph of weight(mg) vs. Temperature for DEA-Ca-Bentonite 40

Figure 45: Graph of derivative weight (%/min) for DEA-Ca-Bentonite..... 41

Figure 46: Graph of weight(%) vs. Temperature for TEA-Ca-Bentonite 41

Figure 47: Graph of weight(mg) vs. Temperature for TEA-Ca-Bentonite..... 43

Figure 481: Graph of derivative weight (%/min) for TEA-Ca-Bentonite 44

LIST OF TABLES

Table 1: General Characteristics of smectites	5
Table 2: Physical Propeties of amines	8
Table 3: Comparison of Infrared Spectra	22
Table 4: Table of % weight loss for Pure Bentonite.....	32
Table 5: Table of % weight loss for Ca-Bentonite	35
Table 6: Table of % weight loss for EA-Ca-Bentonite.....	38
Table 7: Table of % weight loss for DEA-Ca-Bentonite.....	41
Table 8: Table of % weight loss for TEA-Ca-Bentonite	44

CHAPTER 1

INTRODUCTION

1.1 Background

Clays and clay minerals have been mined since the Stone Age; today they are among the most important minerals used by manufacturing and environmental industries. Clay is an abundant raw material which has an amazing variety of uses and properties that are largely dependent on their mineral structure and composition. Basically, Smectite is the group name for several hydrated sodium, calcium, magnesium, iron and lithium aluminium silicates. The individual mineral names in the group are sodium montmorillonite, calcium montmorillonite, magnesium montmorillonite (saponite), iron montmorillonite (nontronite), lithium montmorillonite (hectorite) and aluminium montmorillonite (beidellite). The rock term bentonite is commonly used for these minerals as a clay material altered from a glassy igneous material. Clay is widely chosen as the material for the adsorbent due to its' properties that allows modification of the clays' surface. Besides that, clays allow addition of materials in between of its layers. In this research, the clay was intercalated with organic compound, which are the amines, and surface treated and sent for characterization process.

1.2 Problem Statement

Clay is an abundant raw material which has an amazing variety of uses and properties that are largely dependent on their mineral structure and composition. Unfortunately, these benefits and application is not being utilized optimally. Basically, one special feature that distinguishes clay from other mineral is that clay allows modification of the clays' surface. Besides that, clays allow addition of materials in between of its layers, and this process is better known as Intercalation.

In this research project, this abundant bentonite clay will be intercalated with suitable amine solvents, and amine intercalated clays can be applied in many areas. Therefore with this intercalated clays, further studies can be conducted to develop this intercalated clays into other form of substance such as absorbers, probably to be used in carbon dioxide and heavy metal removal in the industry.

1.3 Objectives and Scope of Study

The main objective of this research is to develop bentonite clay intercalated with various types of amines. The scope of work for this project involves laboratory experiment to which is to produce the intercalated clay, and also to obtain the characterization studies from FT-IR, XRD, SEM and TGA which will give the information on composition morphology and so on.

CHAPTER 2

LITERATURE REVIEW

2.1 Clays and Clay Minerals

Clays are composed essentially of a small group of extremely small crystalline particles of one or more members of a group of minerals that are commonly known as the clay minerals. The clay minerals are hydrous aluminium silicates and in some of these minerals, iron or magnesium substitute for aluminium and in some, there are alkaline and alkaline earth elements present as essential constituents. The term clay is applied to materials having a particle size of less than 2 micrometers. The clay mineral groups are kaolin, smectite, palygorskite-sepiolite, or commonly referred as hornblende, illite, chlorite and mixed layer clays. The properties of these clays are very different, which depends on their structure and composition. For this project, Bentonite clay, or better known as Smectite clay has been chosen as the type of clay that will be used for this research.

2.1.1 Structure and Compositions of Clay Mineral

Grim (1968) suggests that the atomic structure of the clay minerals consists of two basic units, an octahedral sheet and a tetrahedral sheet. The octahedral sheet is comprised of closely packed oxygens and hydroxyls in which aluminium, iron and magnesium atoms are arranged in octahedral coordination. The diagrammatic sketch of the octahedral sheet is shown in figure 1. Another common structural unit is the silica tetrahedral layer in which the silicon atom is equidistant from four oxygen or possibly hydroxyls arranged in the form of tetrahedron with the silicon atom in the centre. These tetrahedrons are arranged to form a hexagonal network repeated infinitely in two horizontal directions to form the silica tetrahedral sheet. The diagrammatic sketch of the tetrahedral sheet is shown in figure 2. Clays are commonly referred to as 1:1 or 2:1. A 1:1 clay would consist of one tetrahedral sheet and one octahedral sheet, and examples would be *kaolinite* and *serpentine*. A 2:1 clay consists of an octahedral sheet sandwiched between two tetrahedral sheets, and examples are *illite*, *smectite*, *attapulgite*, and *chlorite*. The structure and composition of the major industrial clays are very different even though

they are each comprised of octahedral and tetrahedral sheets as their basic component. The different arrangements and composition of the octahedral and tetrahedral sheets account for most of the differences in their physical and chemical properties.

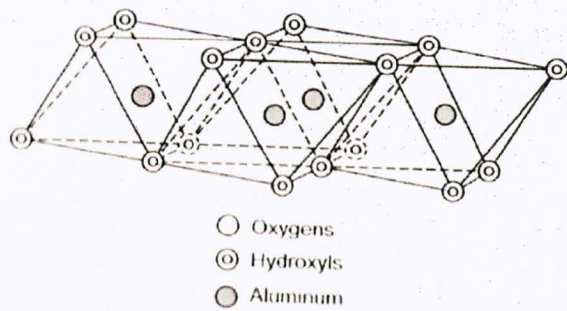


Figure 1: Diagrammatic sketch of the octahedral sheet (Murray, 2007).

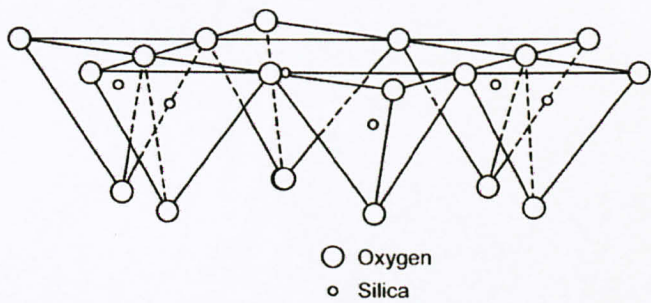


Figure 2: Diagrammatic sketch of the tetrahedral sheet (Murray, 2007).

Smectite minerals are actually consists of 2 silica tetrahedral sheet with a central octahedral sheet, or normally denoted as 2:1 layer mineral (Grim, 1968).

2.1.2 Chemical and Physical Properties of Smectite Clays

According to Murray (2007)

Smectite is the group name for several hydrated sodium, calcium, magnesium, iron and lithium aluminium silicates. The individual mineral names in the group are sodium montmorillonite, calcium montmorillonite, magnesium montmorillonite (saponite), iron montmorillonite (nontronite), lithium montmorillonite (hectorite) and aluminium montmorillonite (beidellite). The rock term bentonite is commonly used for these minerals as a clay material altered from a glassy igneous material, usually volcanic ash. Grim and Guven (1978) used the term bentonite for any clay which was dominantly comprised of a smectite mineral without regard to its origin.

As for the physical characteristics of smectites, Table 1 below summarizes the characteristics of smectites which relates to their applications.

Table 1: General characteristics of smectite

2:1 Layer clay	High sorptive capacity
Variable color, usually tan or greenish-gray	High viscosity
Considerable lattice substitution	Thixotropic
High layer charge	Very low permeability
Medium to high cation exchange capacity	Medium to high swelling capacity
Very fine particle size	High green and dry compression strength
High surface area	High plasticity

2.1.3 Intercalation Behaviour of Montmorillonite into Layered Silicates in Organic Solvents

Numerous studies have illustrates the important need of material clays treated, by some physical and chemical processes, in order to use it as adsorbents. In general, the intercalation of organic into layered phases is conducted by the direct ion exchange of an exchangeable cations, such as Na^+ , K^+ , Ca^{2+} and Mg^{2+} , for inorganic and organic cations. Research proven that the salvation of interlayer amines by solvent molecules will results in the co-intercalation of solvent molecules. The intercalation of a neutral solid amine into H-type layeres phases, for instance H-montmorillonite, can be quantitatively facilitated using organic solvents, as it would appear to help with the diffusion of a solid amine into interlayer. The structure of an interlayer molecular assembly is closely related to the amount of amine intercalated with the interlayer, along with a dependency on the polarity of the organic solvent.

2.2 Comparison of Amine Solutions

The removal of acid gases by the amine process is accomplished by a chemical reaction. Amines can be categorized on a chemical basis as being primary (MEA,DGA) secondary (DEA) and tertiary (MDEA), depending on the number of substituent onto a central Nitrogen element.

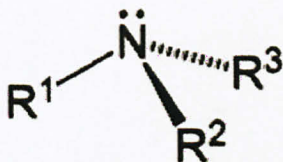


Figure 3: General molecular structure of Amine

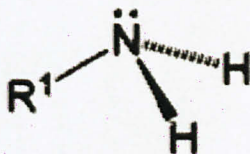


Figure 4: Primary amines

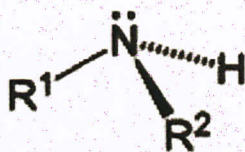


Figure 5: Secondary amines

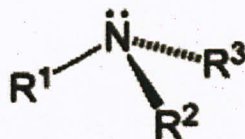


Figure 6: Tertiary amines

2.2.1 Monoethanolamine, MEA

MEA was the first alkanolamine to be used and the process remains essentially unchanged for years. While the predominant use has declined recently, it is often used when the partial pressure of the acid gasses is low, or low acid gas concentration. MEA is a primary amine with the lowest molecular weight. Accordingly, it is the most reactive, volatile and corrosive. It is commonly used in relatively dilute solution, has the highest vaporization losses, require more heat for regeneration and has the lowest hydrocarbon pickup (Perry, 1978).

2.2.2 Diethanolamine, DEA

DEA is also another widely used gas sweetening solvent. Compared to MEA, it has lower heats of reaction with H_2S and CO_2 , is less corrosive, and can be used in higher concentrations with greater acid gas loadings. This will result in a reduced circulation rate and in lower capital and operating costs. Major disadvantages are the inability to slip CO_2 and that some newer processes are more for specific situations. Figure 7 below shows the molecular structure of a typical DEA.

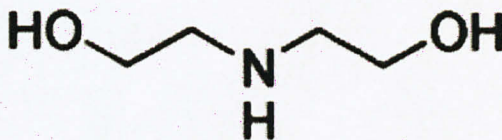


Figure 7: Molecular Structure of DEA

2.2.3 Diglycolamine, DGA

DGA is a primary amine with the same molecular weight as DEA. DGA reduces the circulation rate substantially below that for DEA (Bucklin,1982; Moore et al., 1978). A solution containing 65% DGA freezes at -40°F .this makes DGA very suitable for cold climates. Similarly to MEA, it is suitable for treating gas stream with low partial pressures of acid gasses, and a reclaimer is needed to complete the regeneration. DGA also exhibits a significant affinity for organic compound.

2.2.4 Methyldiethanolamine, MDEA.

MDEA has gained a greater share of the gas treating market in the recent years. MDEA solution have the lowest heat requirement for regeneration because they can be used at 50% strength and acid gas loading of 0.4 mol/mol; have the lowest heats of reaction with CO_2 ; and the lowest specific heat (Pearce,1978 and Daviet et al., 1984). Solvent loses are very low and freezing point is about -25°F . Also MDEA is used in many of the special solvent formulations. Figure below shows the molecular structure of MDEA.



Figure 8: Molecular structure of MDEA.

Table2 below summarizes the physical properties of some primary, secondary and tertiary amines

Table2: Physical properties of amines

Solvent	Specific Gravity	Freezing point ($^{\circ}\text{C}$)	Boiling Point ($^{\circ}\text{C}$)	Molecular Weight
DEA	1.092	28	217	105.14
MEA	1.017	29	170.4	61.08
MDEA	1.040	-21	247	119.16

2.3 Characterization

For the characterization of the intercalated clay, X-Ray Diffraction (XRD), Fourier Transform Infrared Spectroscopy (FTIR), Scanning Electron Microscopy (SEM), Thermogravimetric Analysis (TGA) is used. Studies of structural and morphological characteristic were carried out. XRD studies the nature and behaviour of the crystals. FTIR Spectroscopy studies the nature of bonds. SEM which observes the morphology of particles and last but not least, TGA observes the changes during heating.

2.3.1 X-Ray Diffraction (XRD)

XRD is regularly used to identify the different phases in a polycrystalline sample. Two of its most important advantages for analysis of hybrid materials are that it is fast and nondestructive. When the positions and intensities of the diffraction pattern are taken into account the pattern is unique for a single substance. The X-ray pattern is like a fingerprint and mixtures of different crystallographic phases can easily be distinguished by comparison with reference data. Usually electronic databases such as the Inorganic Crystal Structure database (ICSD) are employed for this comparison. Basically, Solid matter can be described as:

Amorphous: The atoms are arranged in a random way similar to the disorder found in a liquid. For instance, glasses are amorphous materials.

Crystalline: The atoms are arranged in a regular pattern, and there is a smallest volume element that by repetition in three dimensions describes the crystal. This smallest volume element is called a unit cell. The dimensions of the unit cell are described by three axes, which are, **a, b, c** and the angles between them **alpha, beta, gamma**.

The major information that one can get from this method is the crystalline composition and the phase purity. In case of semi crystalline or amorphous materials broad humps are

observed in the diffractogram. Therefore the degree of crystallinity can be qualitatively estimated.

If the crystallites of the powder are very small the peaks of the pattern will broaden. From this broadening it is possible to determine an average crystallite size by the Debye-Scherrer equation:

$$D = \frac{k\lambda}{B \cos \theta}$$

Where k is a factor which is usually set to 0.9, λ is the wavelength of the X-Ray radiation, B is the broadening of the diffraction line measured at half of its maximum intensity (radians) and θ is the Bragg angle. An error for the crystallite size by this formula can be up to 50% which is appropriate. [7]

2.3.2 Scanning Electron Microscopy (SEM)

SEM produces high resolution images of a sample surface. SEM images have a characteristic 3-D appearance and are therefore useful for judging the surface structure of the sample. The primary electrons coming from the source strike the surface and they are inelastically scattered by atoms in the sample. The electrons emitted are detected to produce an image. Beside the emitted electron, X-Rays are also produced by the interaction of electrons with the sample. These can be detected in a SEM equipped for energy dispersive X-Rays (EDX) Spectroscopy. Different detection modes can be applied such as the detection of backscattered electrons or the electron backscatter diffraction (EBSD) which gives crystallographic information about the sample.

The spatial resolution of the SEM techniques depends on various parameters; most of them are instrument related. Generally the resolution goes down to 20nm to 1 nm, which is much lower than that of transmission electron microscopy (TEM) but SEM has some

advantages compared with TEM. For example, a quite large area of specimen can be imaged, bulk materials can be used as samples, and a variety of analytical modes is available for measuring the composition and nature of specimen. [8]. Figure 9 below shows the typical set up of the SEM equipment.

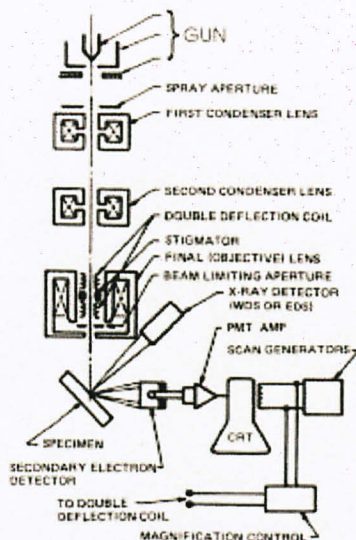


Figure 9: Normal arrangement of SEM equipment. (Egerton, R. F. (2005))

2.3.3 Thermogravimetric Analysis (TGA)

TGA studies the weight changes of samples in relation to changes in temperature. TGA is commonly employed with respect to hybrid materials and nanocomposites to investigate the thermal stability (degradation temperatures), the amount of inorganic component, which usually stays until the end of measurement due to its high thermal resistance, and the level of absorbed moisture or organic volatiles in these materials. Typically TGA plots show the weight lost in relation to the temperature and typical ranges that can be distinguished are the lost of moisture and absorbed solvents up to 150°C, the decomposition of organic components between 300 and 500°C.

Usually the measurements are carried out under air or an inert gas. Listed below are the methodology used during the TGA analysis:

1. A sample of the test material is placed into a high alumina cup that is supported on, or suspended from an analytical balance located outside the furnace chamber.
2. The balance is zeroed, and the sample cup is heated according to a predetermined thermal cycle.
3. The balance sends the weight signal to the computer for storage, along with the sample temperature and the elapsed time.
4. The TGA curve plots the TGA signal, converted to percent weight change on the Y-axis against the reference material temperature on the X-axis.

2.3.4 Fourier Transform Infrared Spectroscopy

Fourier transform infrared (FTIR) spectroscopy is a measurement technique for collecting infrared spectra. Instead of recording the amount of energy absorbed when the frequency of the infra-red light is varied (monochromator), the IR light is guided through an interferometer. After passing through the sample, the measured signal is the interferogram. Performing a mathematical Fourier transform on this signal results in a spectrum identical to that from conventional (dispersive) infrared spectroscopy.

FTIR spectrometers are cheaper than conventional spectrometers because building of interferometers is easier than the fabrication of a monochromator. In addition, measurement of a single spectrum is faster for the FTIR technique because the information at all frequencies is collected simultaneously. This allows multiple samples to be collected and averaged together resulting in an improvement in sensitivity. Because of its various advantages, virtually all modern infrared spectrometers are FTIR instruments. The normal instrumental process is as follows [9]:

1. **The Source:** Infrared energy is emitted from a glowing black-body source. This beam passesthrough an aperture which controls the amount of energy presented to the sample (and, ultimately,to the detector).
2. **The Interferometer:** The beam enters the interferometer where the “spectral encoding” takesplace. The resulting interferogram signal then exits the interferometer.
3. **The Sample:** The beam enters the sample compartment where it is transmitted through or reflected off of the surface of the sample, depending on the type of analysis being accomplished. This is where specific frequencies of energy, which are uniquely characteristic of the sample, are absorbed.
4. **The Detector:** The beam finally passes to the detector for final measurement. The detectors used are specially designed to measure the special interferogram signal.
5. **The Computer:** The measured signal is digitized and sent to the computer where the Fourier transformation takes place. The final infrared spectrum is then presented to the user for interpretation and any further manipulation. Figure 10 below shows the graphical overall process that takes place during FTIR.

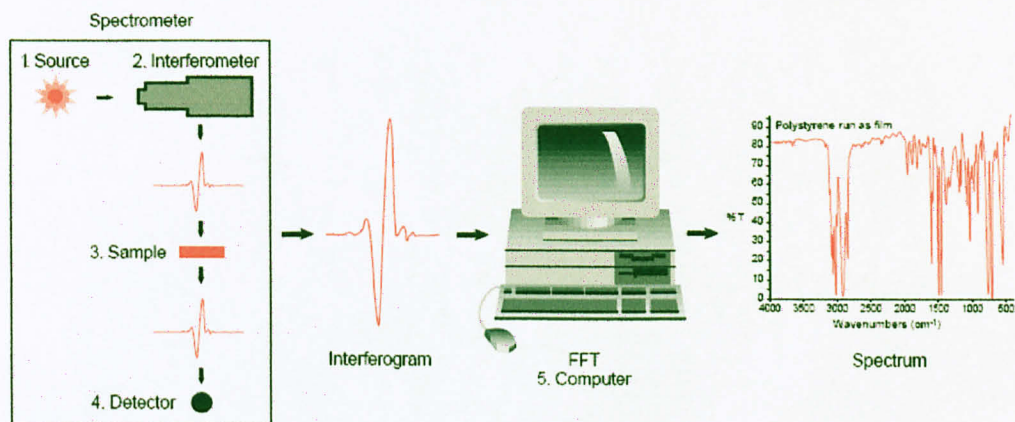


Figure 10: Overall FTIR process (Thermo Nicolet, 2001)

2.4 Cation Exchange Capacity (CEC)

In soil science, cation exchange capacity (CEC) is the capacity of a soil for ion exchange of Cations between the soil and the soil solution. CEC is used as a measure of fertility, nutrient retention capacity, and the capacity to protect groundwater from cation contamination. Cations can also be easier to understand by just adding the group number.

The quantity of positively charged ions (cations) that a clay mineral or similar material can accommodate on its negatively charged surface is expressed as milli-ion equivalent per 100 g, or more commonly as milliequivalent (meq) per 100 g. Clays are luminosity in which some of the aluminium and silicon ions have been replaced by elements with different valence, or charge. For example, aluminium (Al^{3+}) may be replaced by iron (Fe^{2+}) or magnesium (Mg^{2+}), leading to a net negative charge. This charge attracts cations when the clay is immersed in an electrolyte such as salty water and causes an electrical double layer. The cation-exchange capacity is often expressed in terms of its contribution per unit pore volume, Q_v . Mathematically it can be expressed as following:

$$CEC = \frac{100 \text{ mEq of cation}}{100 \text{ g of clay}}$$

CHAPTER 3

METHODOLOGY

3.1 Experimental Procedures

1. Preparation of Clay Suspension:

About 10g of pure bentonite clay was placed in a conical flask and 150ml of distilled water was added. This flask was sealed and stirred overnight on a mechanical stirrer to ensure the dispersion of the clay, as shown by the figure below:



Figure 11 : Stirring process of the clay slurry

2. Preparation of Calcium Bentonite:

About 500 ml of 1M CaCl was added to the clay slurry and shaken overnight. The mixture was then preheated to about 65°C so as to get a complete ion exchange of clay. The resulting suspension was centrifuged at 2000 rpm for 30 minutes and the supernatant layer was collected in a beaker. This process was repeated several times. The clay slurry was transferred to dialysis tubing and chloride ions were removed by repeated dialysis with deionized water. The clay samples were then dried in an oven at 100°C for 3 hours.

3. Preparation of Modified Bentonite:

Previously dried and desiccated calcium bentonite clay was mixed with amine for which the concentration will be 5mEq greater than CEC of bentonite clay. The mixture was subjected to mechanical shaking for 48 hours at a constant temperature of 25°C. The clay suspension was then be separated from the mixture by centrifugation, washed with distilled water, dried at 40°C for 24 hours and mechanically ground to produce fine powder.

4. Characterization of modified clays

The BET surface area was determined by nitrogen adsorption at 77 K in a StrOhlen Areameter. Thermogravimetric Analyses (TGA) were carried out on samples weighing under a flow of N₂ (10 mL min⁻¹) at a heating rate of 15°C min⁻¹. The XRD powder profiles were obtained with a Siemens D-500 diffractometer using nickel filtered CuK α radiation. The FT-IR spectra of samples were recorded in KBr (1mg sample/ 250 mg KBr) pellets using MAIDAC 1700M FTIR Spectrometer in the range of 4000-400 cm⁻¹ with a resolution of 2cm⁻¹ after 50 scan. Scanning Electron Micrograph (SEM) pictures were obtained with a result of particle size diameter and surface area at different magnifications.

CHAPTER 4

RESULTS AND DISCUSSION

4.1 Synthesis of Amine-Intercalated Ca-Bentonite

Figures 12 and 13 shows the 2 layers of clay and supernatant produced from the centrifuge process and the supernatant liquid collected in a beaker, respectively.

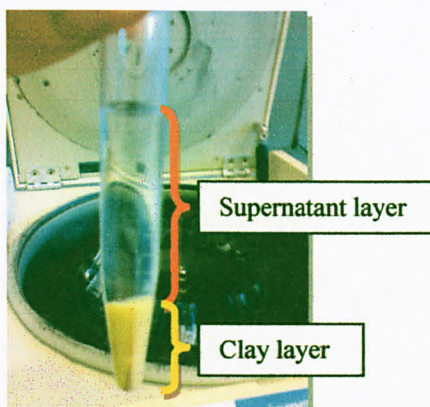


Figure 12: The results from the centrifuge process



Figure 13: The supernatant layers collected in a beaker for calcium testing

Drying process

After separating the supernatant and the clay layer from the centrifuge, the clay layer is collected and placed in an oven at 100°C for almost 3 hours. This process will give us dried sodium bentonite clay. The dried samples were then sent for grinding and the result is shown in figure 14.

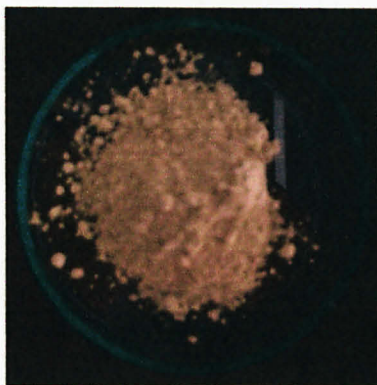


Figure 14: The dried Bentonite Clay.

Listed below are the prepared samples which will be sent for characterization:

- i) Pure Bentonite
- ii) Ca-Bentonite
- iii) Ca-Bentonite intercalated with Ethanolamine
- iv) Ca-Bentonite intercalated with Diethylamine
- v) Ca-Bentonite intercalated with Triethylamine

Figure 15 below shows the samples stored in the laboratory to be sent for various characterizations.



Figure15: Prepared Samples

4.2 Characterization of Amine-Intercalated Ca-Bentonite

4.2.1 Fourier Transform Infrared Spectroscopy (FTIR)

The FTIR spectra of montmorillonite and different organic complexes exchanged onto montmorillonite were obtained in the region $4000\text{--}400\text{cm}^{-1}$ with a resolution of 2cm^{-1} from a MAIDAC 1700M FTIR Spectrometer dispersed in KBr (1mg sample/250mg KBr) pellets. IR data are gathered in Tables 3. The characteristic peaks of the montmorillonite and cations exchanged montmorillonite used in this study and the detailed vibrational frequencies with possible assignments being given are obtained from studies. All products exhibit two moderately intense bands in the range of between $3620.14 - 3697.29\text{ cm}^{-1}$, which might be ascribed to the stretching frequencies of the OH^- functional groups of free molecules of water. The intensity bands ranging from $3420.12 - 3448.49\text{ cm}^{-1}$ on the other hand, indicates the stretching frequencies of OH^- functional groups of bonded water. For all of the samples, the most intense IR band occur in 875.62 cm^{-1} which corresponds to the Si-O and Si-O-Si vibrations and due to the greater ionic character of the Si-O group.

The most important part to be highlighted is N-H bending indicated by intensity bands ranging from $1562.87 - 1631.02$ and C-N stretching indicated by intensity bands ranging from $1323.08 - 1407.94$ for all three amine-intercalated samples; EA-Intercalated, DEA-Intercalated and TEA-Intercalated Na-Bentonite only. These two assignments are the fingerprint group of amine functional group.

The table below shows the comparison of intensities between all 5 samples:

Table 3: Comparison of infrared spectra

Pure Bentonite	Ca-Bentonite	EA-Intercalated Ca-Bentonite	DEA-Intercalated Ca-Bentonite	TEA-Intercalated Ca-Bentonite	Peak Assignment
3697.29 - 3620.14	3695.36 - 3620.14	3695.30	3695.36 – 3652.93	3695.36 – 3620.14	OH functional group of co-ordinated water; OH ⁻ stretching of free water
3448.49	3569.99-3423.41	-	-	3380.10 – 3360.0	OH ⁻ stretching of bonded water
-	-	3442.70 – 3419.56			Stretching of N-H
-	2856.38	-	2956.67	2958.60 – 2931.60	Stretching of C-H
-	-	-	2893.02	2830.88-2761.58	Stretching: ν (C-N)
2360.71 - 2339.49	2378.07 – 2136.98	-	2362.64 – 2032.83	-	Phenyl ring stretching
1641.31	1637.45	-	-	-	δ (H ₂ O) deformation
-	-	-	1627.81	-	Bending of N-H
1465.80	-	1477.37	1477.37-1461.94	-	Stretching of C-C
-	-	-	-	-	Stretching of C-N
-	-	1010.6	-	-	Bending of C-N
1044.42	1025.20	-	1030.10	-	Stretching vibration of Si-O, Si-O-Si and Al-O
912.27	914.20	-	912.27	-	OH deformation attached to Fe ³⁺ , Al ³⁺ and Mg ²⁺
875.62	877.55	-	873.69	-	Stretching vibration of Si-O, Si-O-Si and Al-O
794.62 - 756.04	796.55 - 754.12	-	796.55 – 781.12	-	Silica quartz impurity
692.40 - 532.32	692.40-530.39	541.96	694.33 - 540.39	-	Si-O deformation
466.74 – 428.17	480.74 – 426.24	-	461.71 – 420.24	-	Al-O Stretching

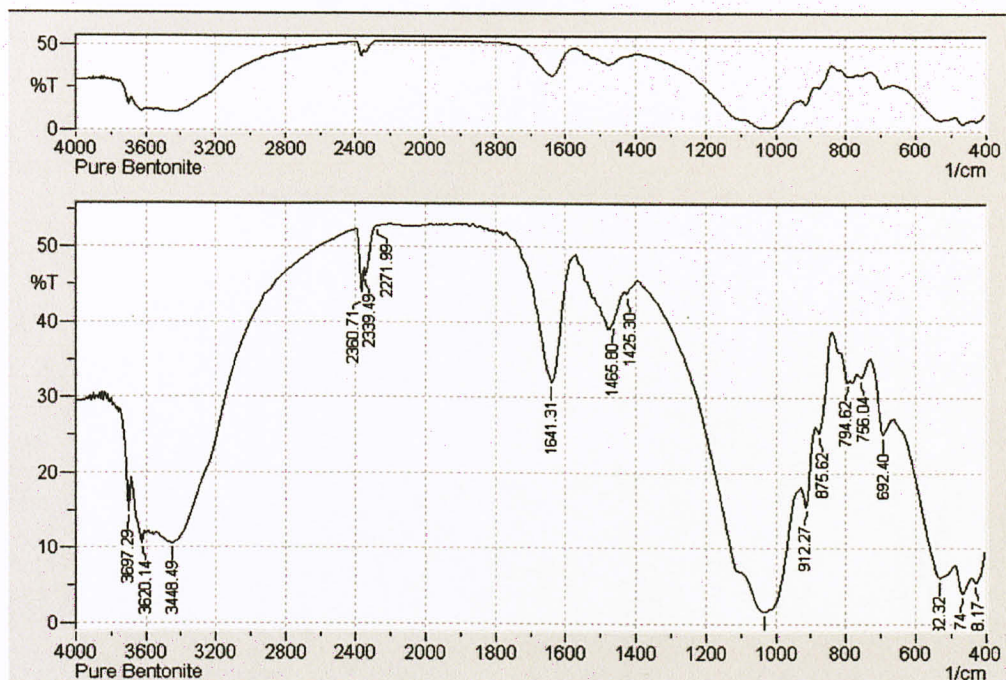


Figure 16: FTIR Image for Pure Bentonite

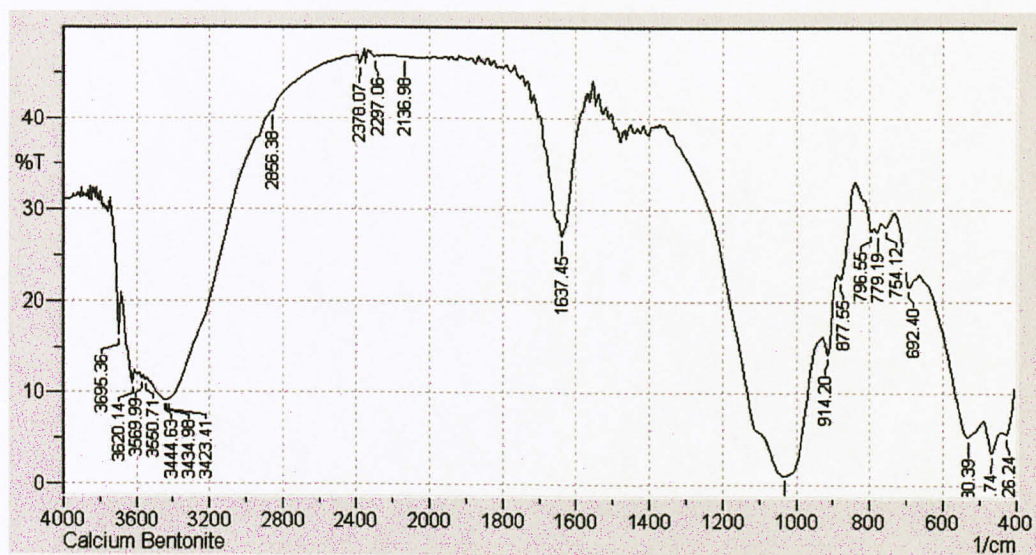


Figure 17: FTIR Image for Ca-Bentonite

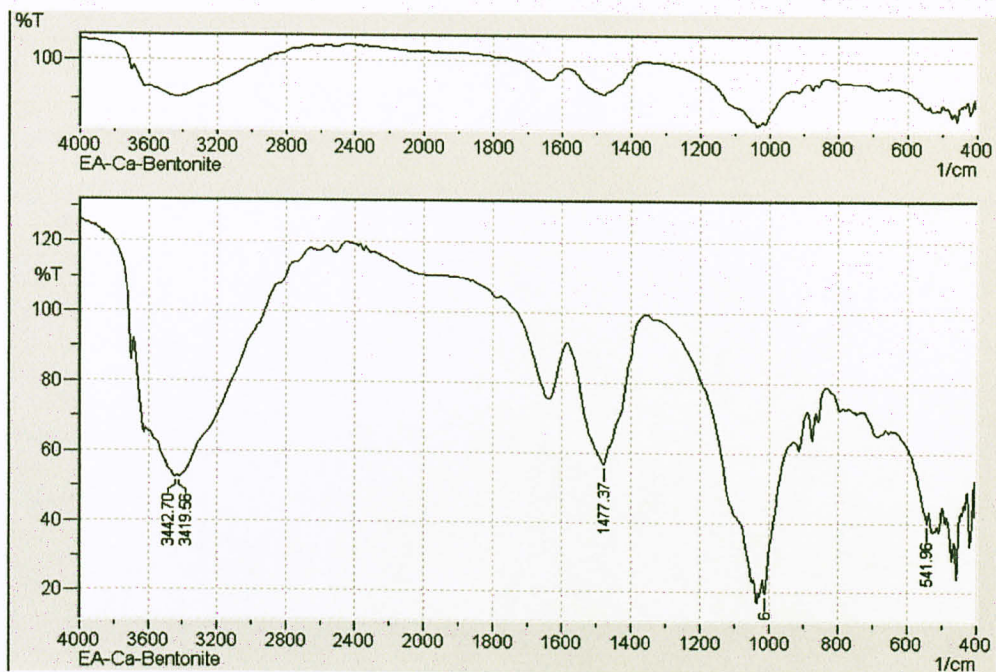


Figure 18: FTIR Image for EA-Intercalated Ca-Bentonite

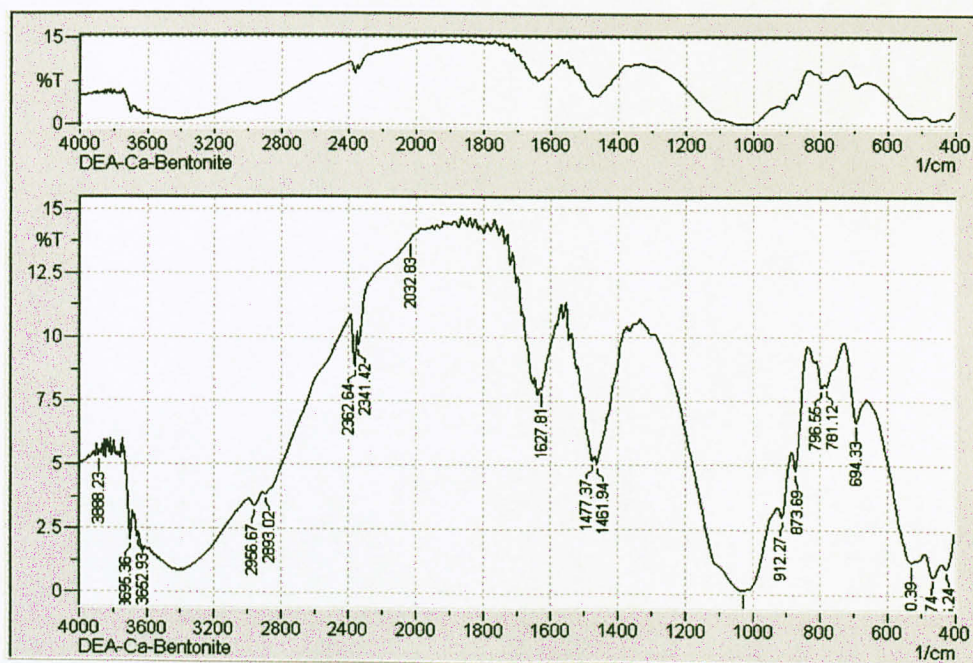


Figure 19: FTIR Image for DEA-Intercalated for Ca-Bentonite

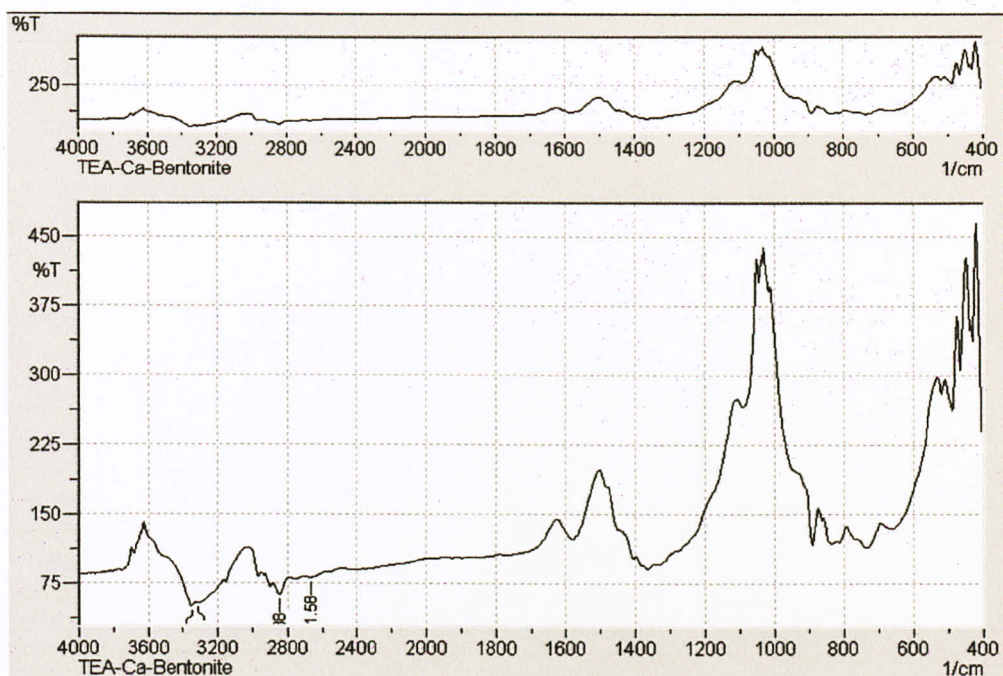


Figure 20: FTIR Image for TEA-Intercalated Ca-Bentonite

4.2.2 X-ray Diffraction (XRD)

X-ray diffraction patterns were obtained using a Siemens D-500 diffractometer equipped with nickel filtered Cu-K α radiation (40kV, 30 mA). The X-ray diffraction patterns of the sample clay confirm the characteristics of montmorillonite type. It shows quartz impurities, residues of feldspar and traces of limestone are present.

The basal spacing (d) of the component of concern; *Montmorillonite*, *syn* – $Al_2O_3 \cdot 4SiO_2 \cdot xH_2O$ (green colour) is observed to increase after the intercalation of amine. This increment can be seen from the drastic hike in the intensity for all of the 3 samples intercalated with amine as indicated in the figures 21 to 25 below. The red coloured dash-lined circle shows the intensities before and after intercalation. It can be seen that the most drastical increase in intensity is in the sample TEA-Intercalated Ca-Bentonite.

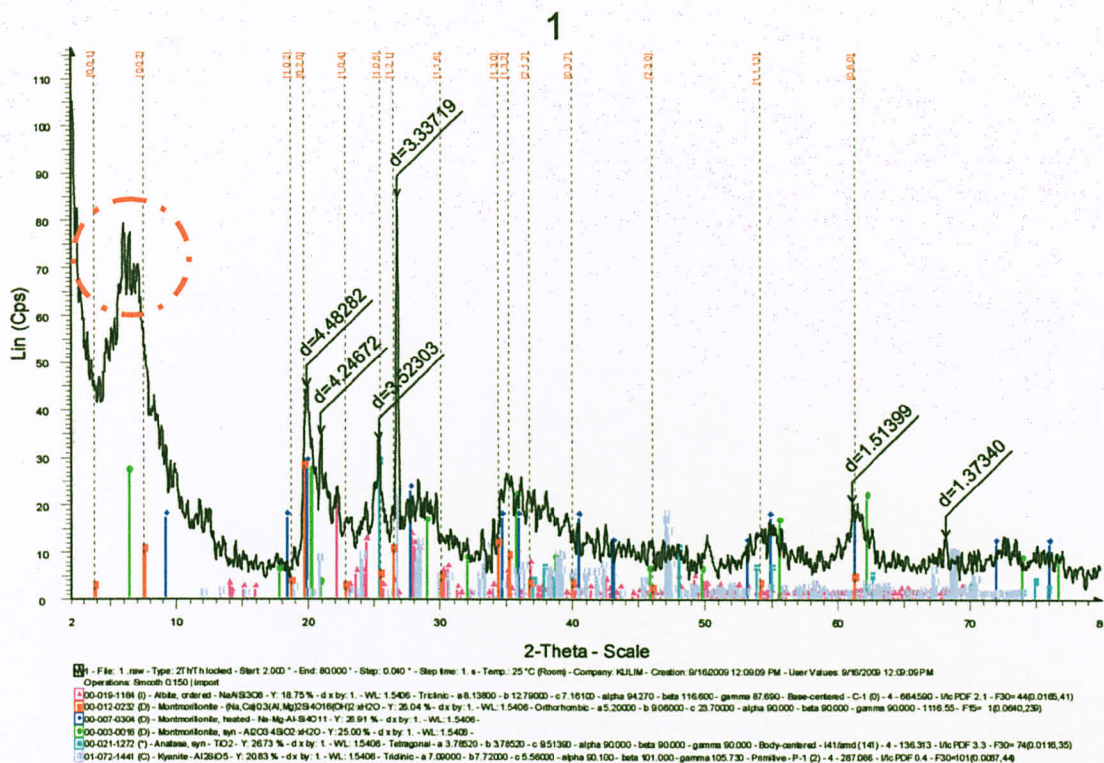


Figure 21: XRD Image of Pure Bentonite

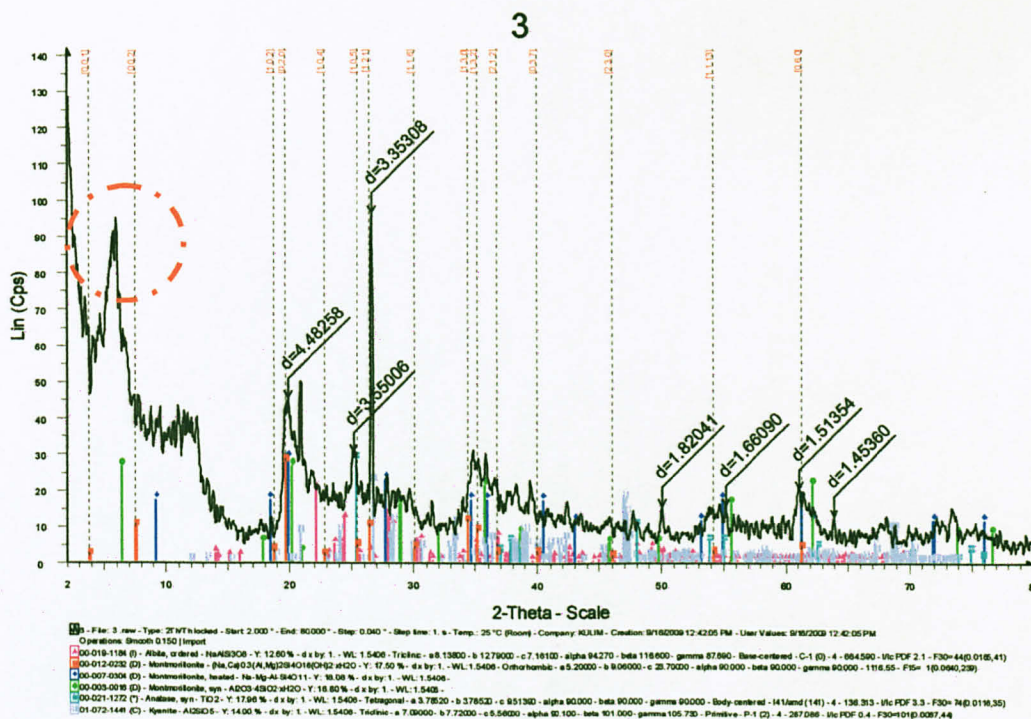


Figure 22: XRD Image of Ca-Bentonite

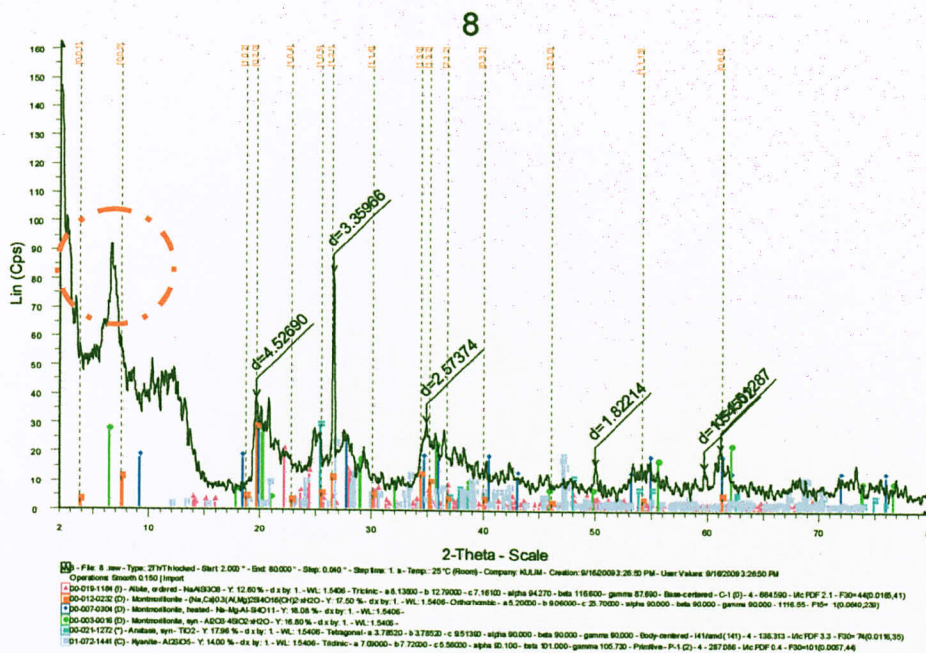


Figure 23: XRD Image of EA-Intercalated Ca-Bentonite

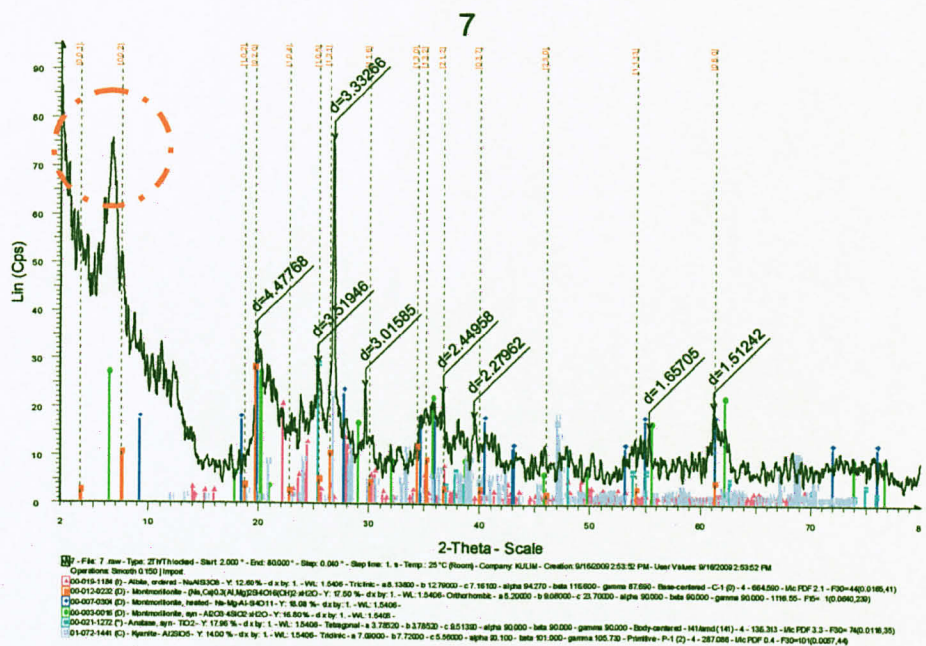


Figure 24: XRD Image of DEA-Intercalated Ca-Bentonite

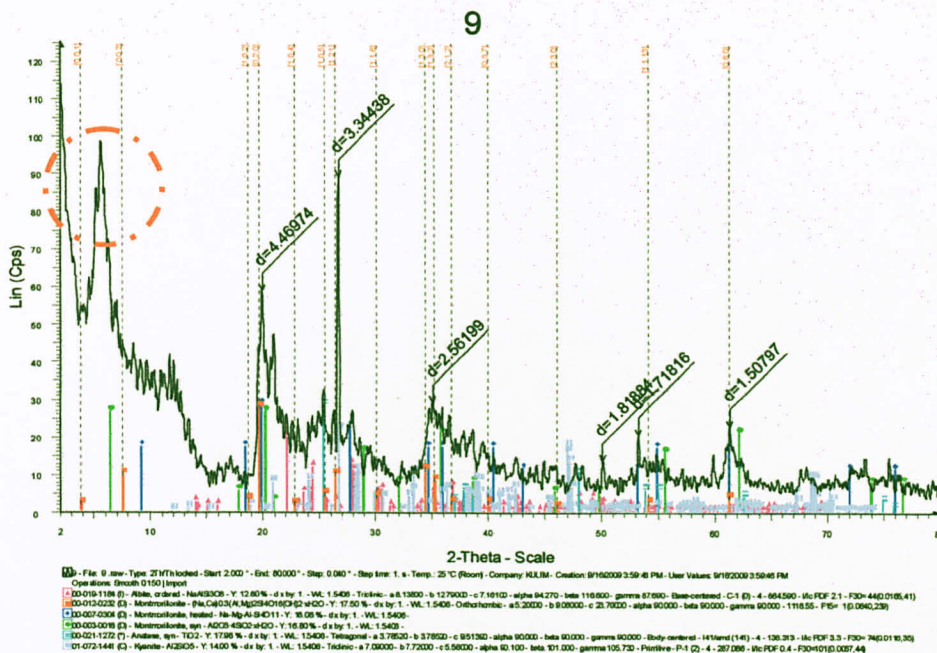


Figure 25: XRD Image of TEA-Intercalated Ca-Bentonite

4.2.3 Scanning Electro Microscopy (SEM)

Scanning Electro Microscopy provides us with the high resolution image of the sample surface. In our case, we magnified the sample surface to 5000 times and 100 times magnification. From that, we can observe the surface topography; its pore size, particle size, as well as the coagulation of the particles.

The figures below show the comparison of SEM images for Pure Bentonite and other intercalated Ca-Bentonite samples:

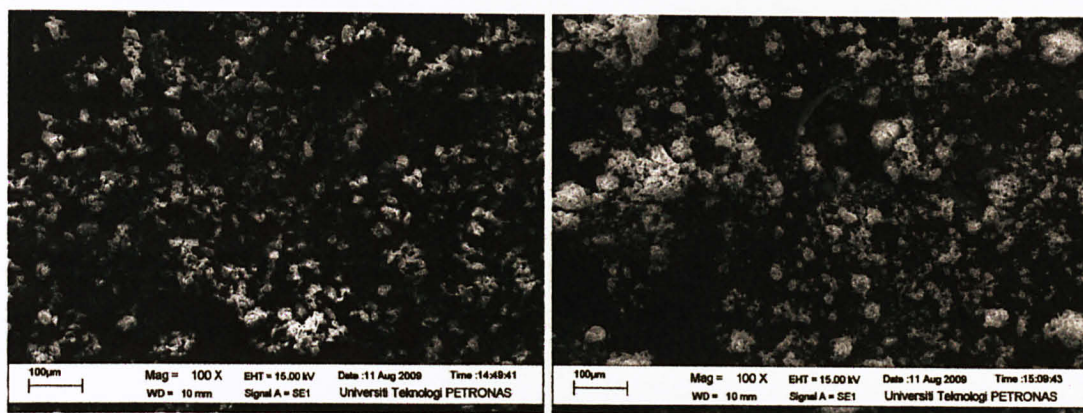


Figure 26: Comparison of SEM Images between Pure Bentonite (left) and Ca-Bentonite (right) at 100x Magnification

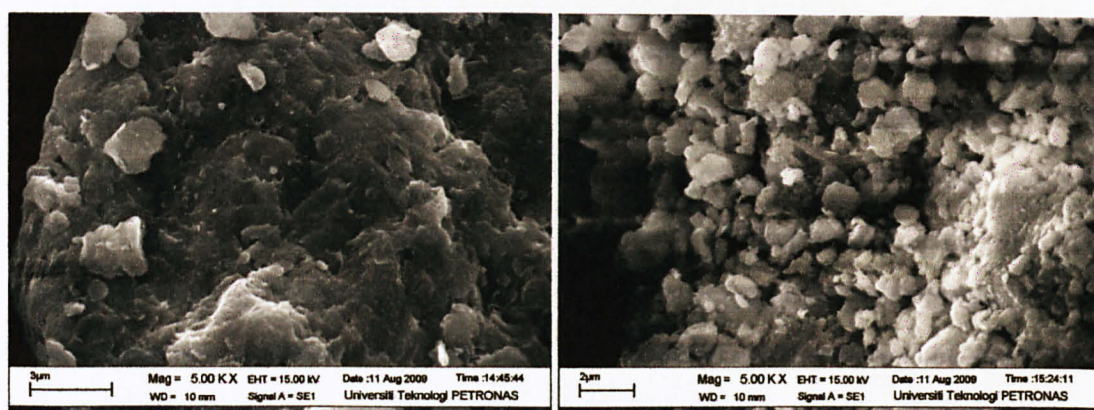


Figure 27: Comparison of SEM Images between Pure Bentonite (left) and Ca-Bentonite (right) at 5000x Magnification

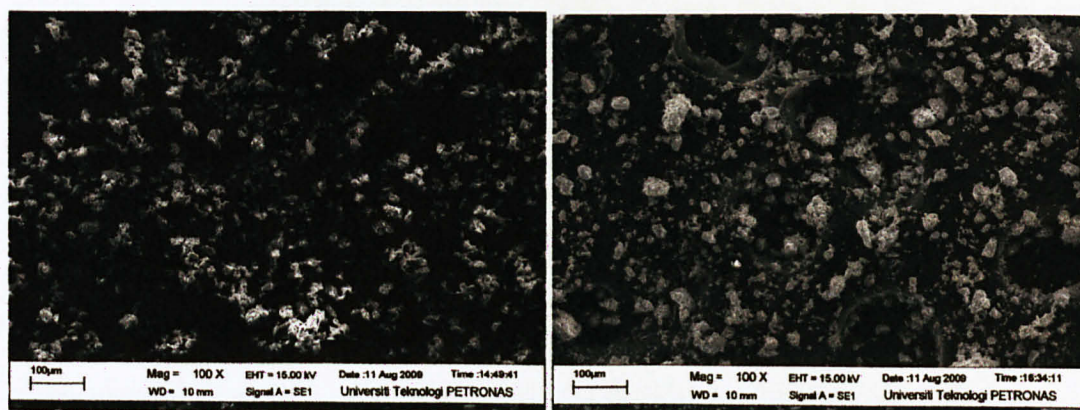


Figure 28: Comparison of SEM Images between Pure Bentonite (left) and EA-Intercalated Ca-Bentonite (right) at 100x Magnification

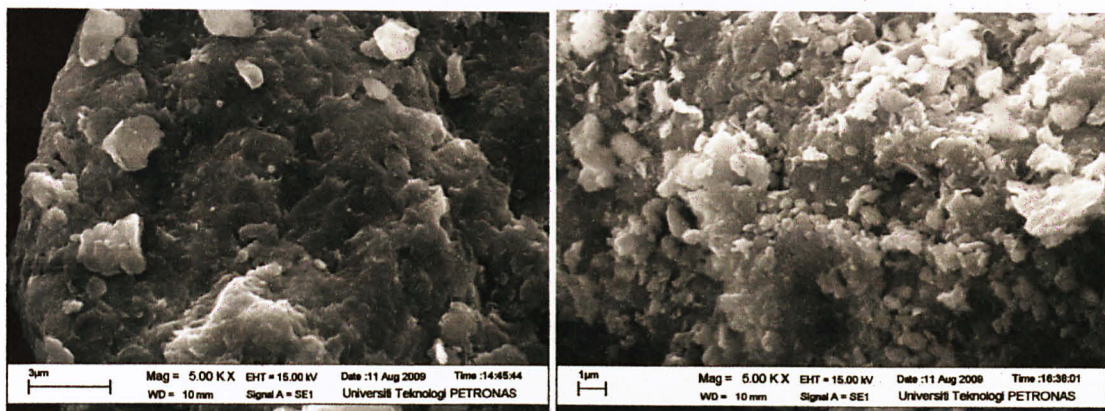


Figure 29: Comparison of SEM Images between Pure Bentonite (left) and EA-Intercalated Ca-Bentonite (right) at 5000x Magnification

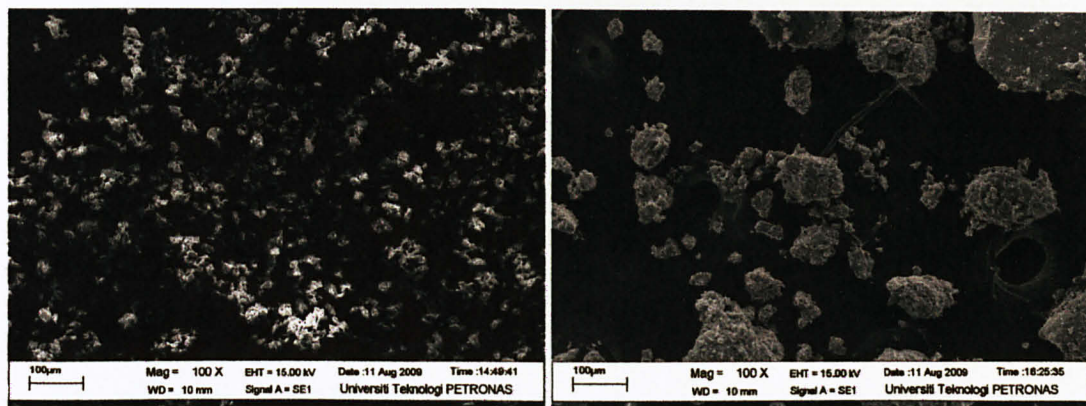


Figure 30: Comparison of SEM Images between Pure Bentonite (left) and DEA-Intercalated Ca-Bentonite (right) at 100x Magnification

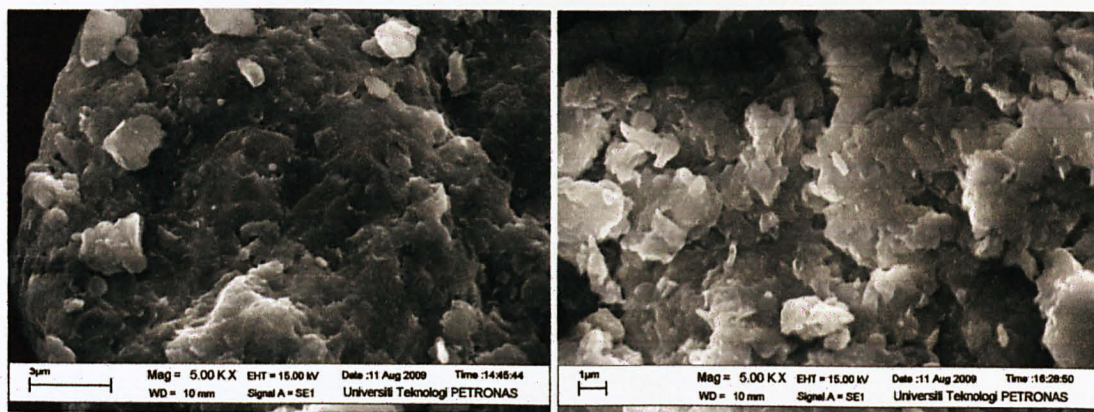


Figure 31: Comparison of SEM Images between Pure Bentonite (left) and DEA-Intercalated Ca-Bentonite (right) at 5000x Magnification

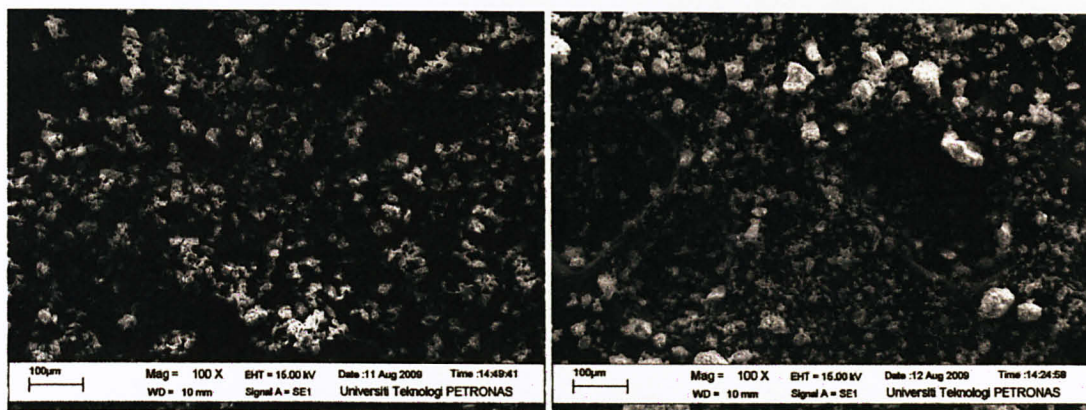


Figure 32: Comparison of SEM Images between Pure Bentonite (left) and TEA-Intercalated Ca-Bentonite (right) at 100x Magnification

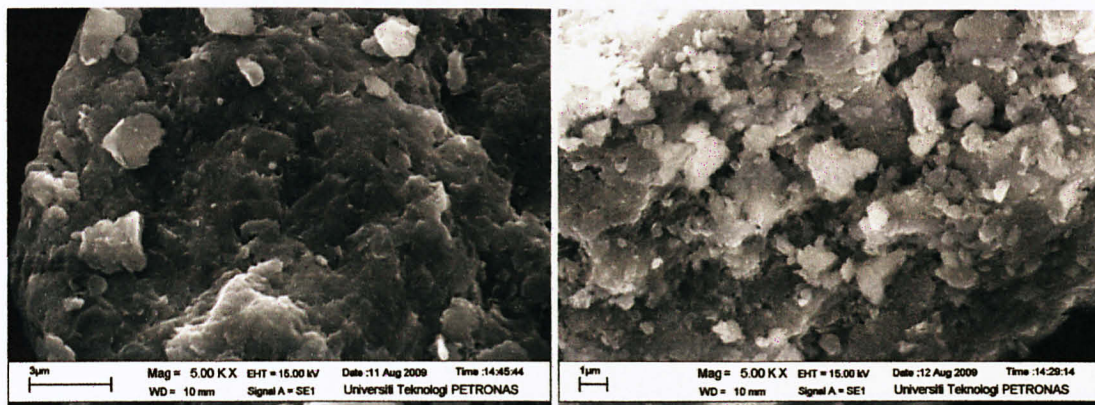


Figure 33: Comparison of SEM Images between Pure Bentonite (left) and TEA-Intercalated Ca-Bentonite (right) at 5000x Magnification

4.2.4 Thermogravimetric Analysis (TGA)

Table 4 below shows the weight loss of Pure Bentonite sample as the temperature is increased 15°C/min in increment of 10°C in the range of 50-900°C.

Table 4: Table of Percentage Weight Loss for Pure Bentonite

Temperature (°C)	Weight % (%)
49.56	99.962
59.56	99.534
69.56	98.929
79.56	98.116
89.56	97.329
99.56	96.867
109.56	96.655
119.56	96.534
129.56	96.442
139.56	96.376
149.56	96.332
159.56	96.284
169.56	96.24
179.56	96.199
189.56	96.161
199.56	96.125
209.56	96.086
219.56	96.05
229.56	96.01
239.56	95.97
249.56	95.928
259.56	95.881
269.56	95.83
279.56	95.771
289.56	95.729
299.56	95.691
309.56	95.657
319.56	95.622
329.56	95.584
339.56	95.543
349.56	95.492
359.56	95.449
369.56	95.398
379.56	95.329
389.56	95.258
399.56	95.167
409.56	95.051
419.56	94.909
429.56	94.728
439.56	94.53

Temperature (°C)	Weight % (%)
449.56	94.288
459.56	94.004
469.56	93.664
479.56	93.264
489.56	92.803
499.56	92.309
509.56	91.805
519.56	91.355
529.56	91.021
539.56	90.782
549.56	90.617
559.56	90.481
569.56	90.361
579.56	90.249
589.56	90.14
599.56	90.03
609.56	89.921
619.56	89.809
629.56	89.696
639.56	89.579
649.56	89.461
659.56	89.361
669.56	89.285
679.56	89.241
689.56	89.221
699.56	89.212
709.56	89.205
719.56	89.207
729.56	89.219
739.56	89.235
749.56	89.255
759.56	89.269
769.56	89.284
779.56	89.297
789.56	89.309
799.56	89.324
809.56	89.341
819.56	89.36
829.56	89.384
839.56	89.409

Temperature (°C)	Weight % (%)
849.56	89.425
859.56	89.454
869.56	89.486
879.56	89.499
889.56	89.546

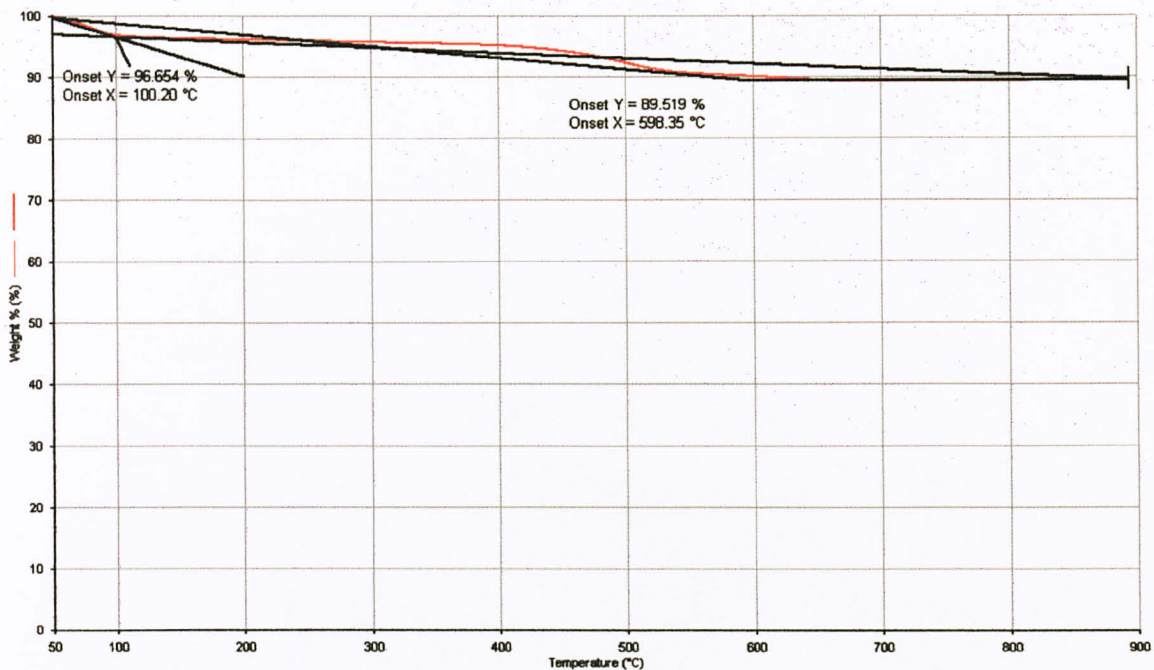


Figure 34: Graph of Weight Percentage (%) vs. Temperature (°C) for Pure Bentonite

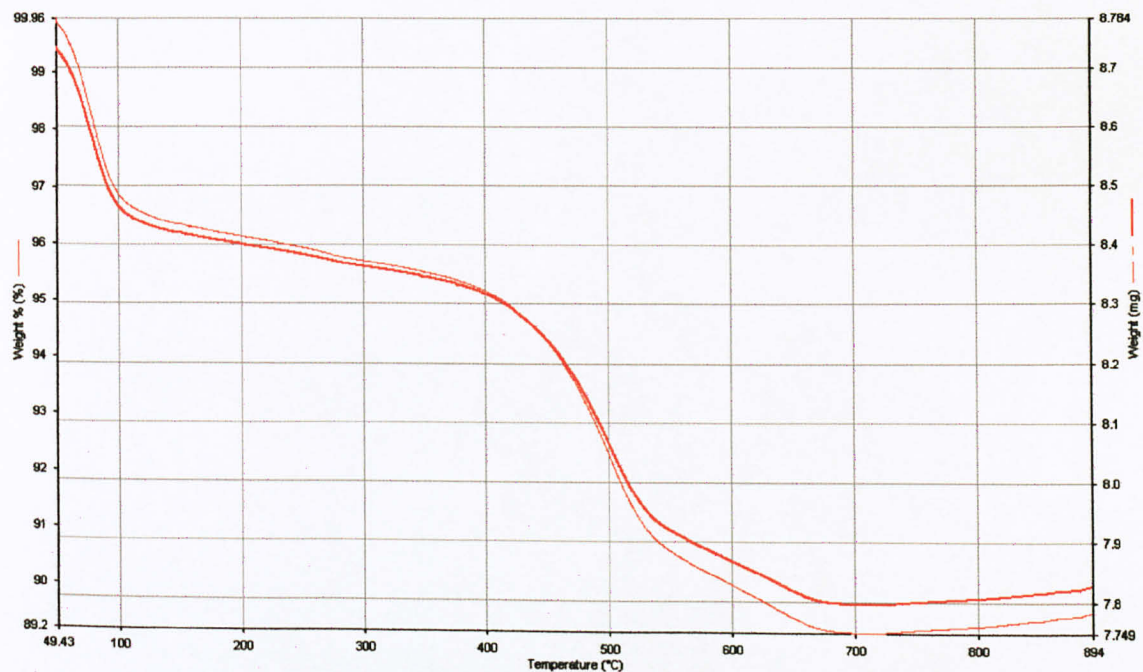


Figure 35: Graph of Weight (mg) vs. Temperature (°C) for Pure Bentonite

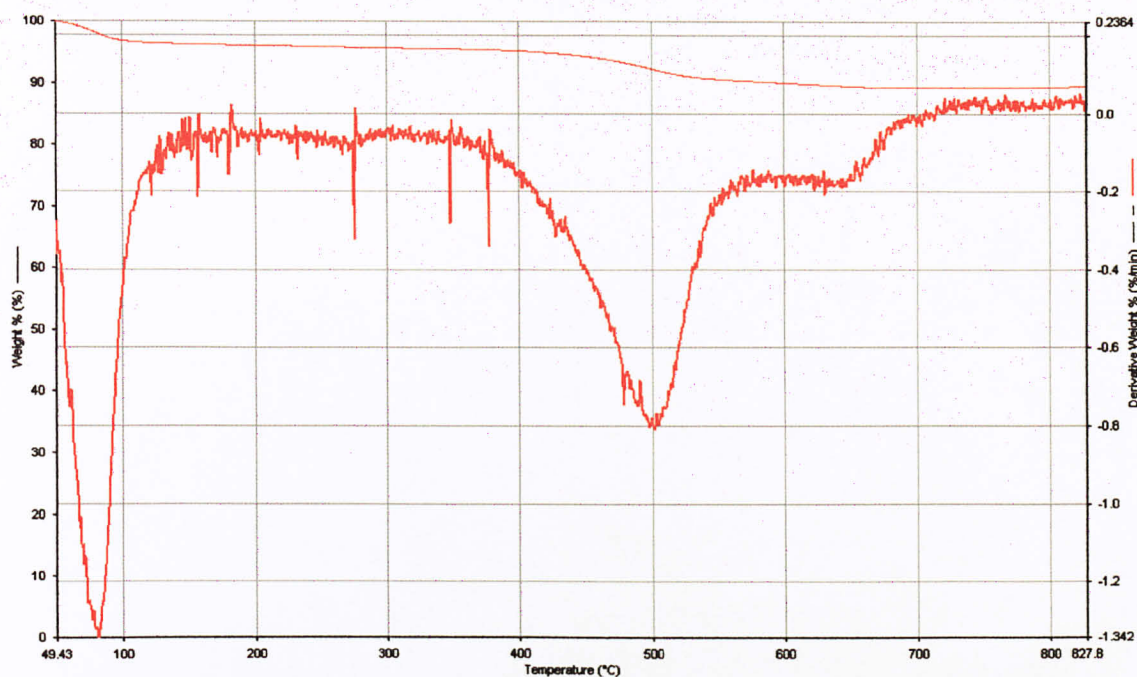


Figure 36: Graph of Derivative Weight (%/min) vs. Temperature (°C) for Pure Bentonite

From these graphs, we can see that at $T=100^{\circ}\text{C}$, there's weight loss attributed to the desorption of physically adsorbed natural water. At $T=500^{\circ}\text{C}$, there is also some weight loss observed, and this is attributed to the desorption of structural water due to the dehydroxillation of the layered aluminosilicate.

Table 5 below shows the weight loss of Ca-Bentonite sample as the temperature is increased $15^{\circ}\text{C}/\text{min}$ in increment of 10°C in the range of $50\text{--}900^{\circ}\text{C}$.

Temperature (°C)	Weight % (%)
49.49	99.969
59.49	99.527
69.49	98.927
79.49	98.149
89.49	97.337
99.49	96.61
109.49	96.026
119.49	95.565
129.49	95.155
139.49	94.784
149.49	94.429
159.49	94.148
169.49	93.982
179.49	93.873
189.49	93.79
199.49	93.715
209.49	93.645
219.49	93.583
229.49	93.521
239.49	93.461
249.49	93.396
259.49	93.325
269.49	93.25
279.49	93.167
289.49	93.084
299.49	93.012
309.49	92.948
319.49	92.882

Temperature (°C)	Weight % (%)
329.49	92.812
339.49	92.739
349.49	92.658
359.49	92.568
369.49	92.474
379.49	92.367
389.49	92.251
399.49	92.114
409.49	91.964
419.49	91.782
429.49	91.573
439.49	91.336
449.49	91.078
459.49	90.764
469.49	90.41
479.49	90.018
489.49	89.584
499.49	89.126
509.49	88.688
519.49	88.319
529.49	88.036
539.49	87.837
549.49	87.688
559.49	87.57
569.49	87.469
579.49	87.378
589.49	87.295
599.49	87.215
609.49	87.139

Temperature (°C)	Weight % (%)
619.49	87.072
629.49	87.01
639.49	86.952
649.49	86.897
659.49	86.85
669.49	86.809
679.49	86.767
689.49	86.732
699.49	86.702
709.49	86.672
719.49	86.649
729.49	86.624
739.49	86.608
749.49	86.594
759.49	86.582
769.49	86.571
779.49	86.566
789.49	86.561
799.49	86.56
809.49	86.562
819.49	86.566
829.49	86.573
839.49	86.588
849.49	86.607
859.49	86.63
869.49	86.66
879.49	86.693
889.49	86.737

Table 5: Table of Percentage Weight Loss for Ca-Bentonite

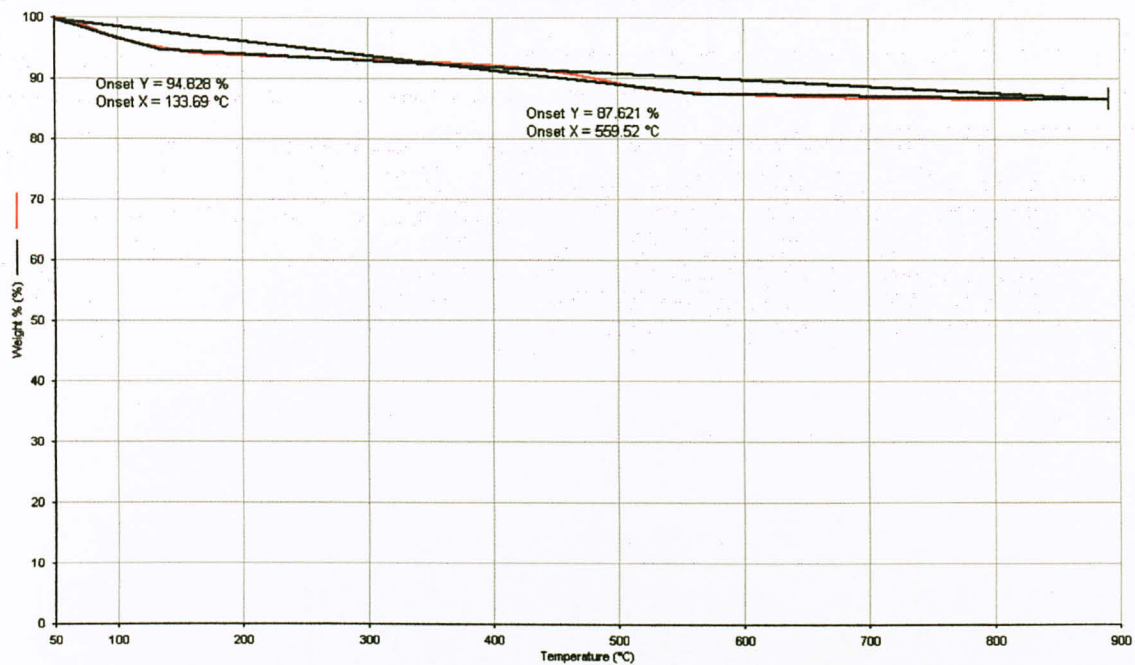


Figure 37: Graph of Weight Percentage (%) vs. Temperature (°C) for Ca-Bentonite

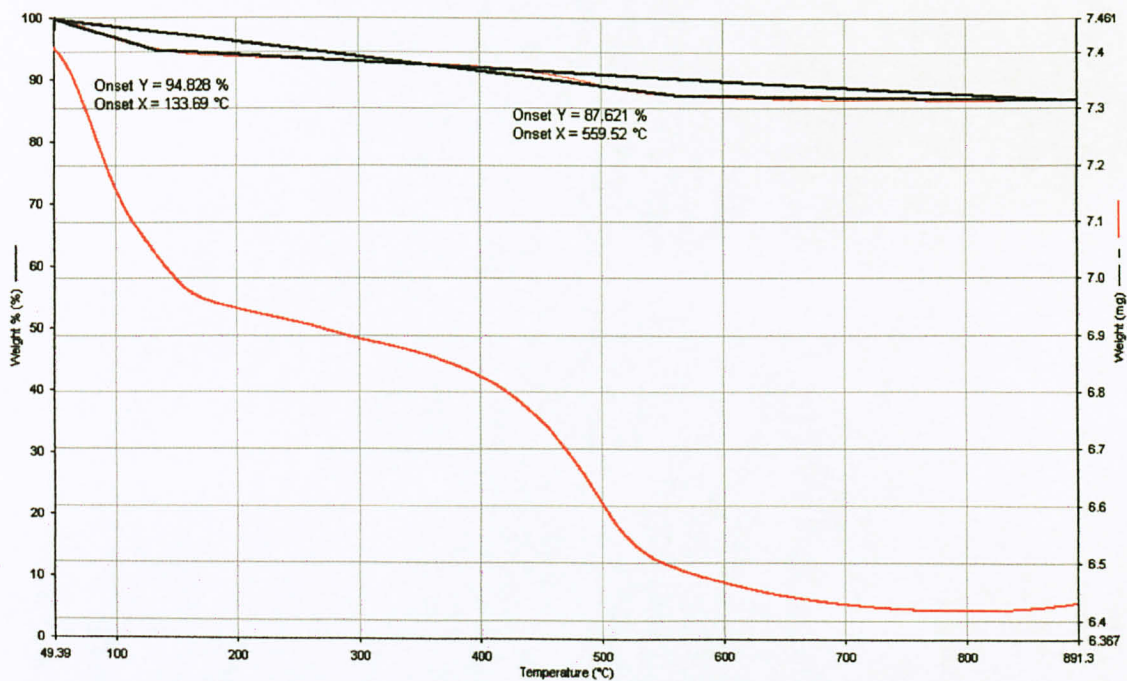


Figure 38: Graph of Weight (mg) vs. Temperature (°C) for Na-Bentonite

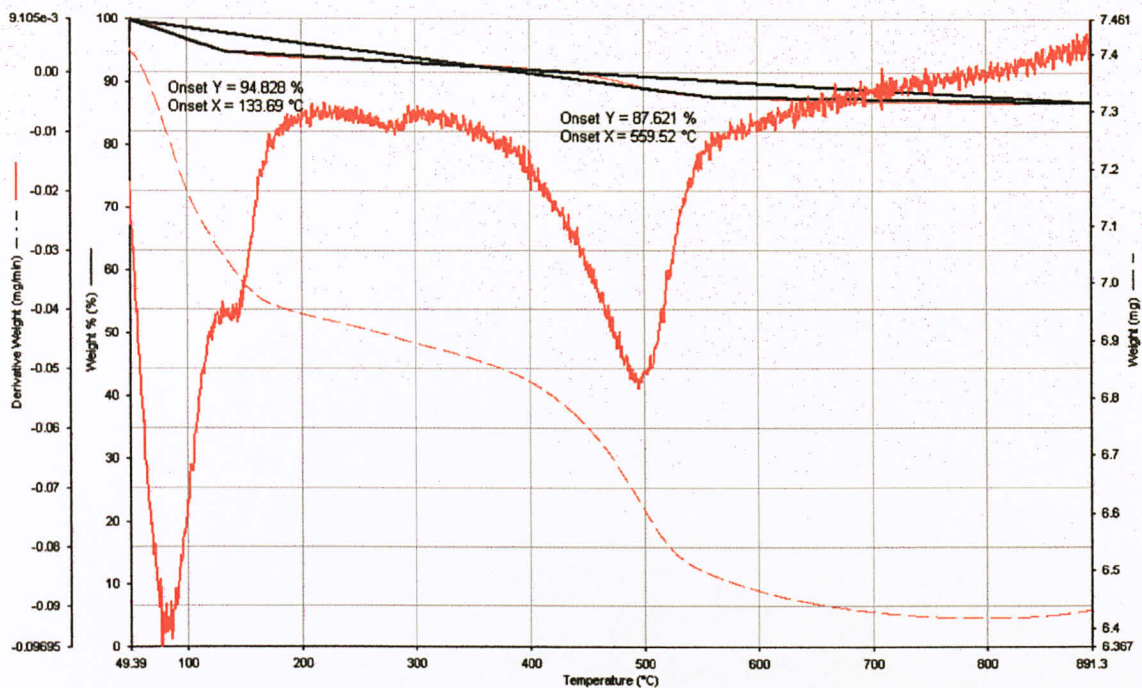


Figure 39: Graph of Derivative Weight (%/min) vs. Temperature (°C) for Ca-Bentonite

From these graph also, we can see that at $T=100^{\circ}\text{C}$, there's weight loss attributed to the desorption of physically adsorbed natural water. At $T=500^{\circ}\text{C}$, there is also some weight loss observed, and this is attributed to the desorption of structural water due to the dehydroxillation of the layered aluminosilicate.

Table 6 shows the weight loss of EA-Intercalated Ca-Bentonite sample as the temperature is increased $15^{\circ}\text{C}/\text{min}$ in increment of 10°C in the range of $50\text{-}900^{\circ}\text{C}$.

Table 6: Table of Percentage Weight Loss for EA-Intercalated Ca-Bentonite

Temperature (°C)	Weight % (%)
49.56	99.772
59.56	98.969
69.56	98.163
79.56	97.382
89.56	96.755
99.56	96.333
109.56	96.045
119.56	95.829
129.56	95.662
139.56	95.543
149.56	95.449
159.56	95.366
169.56	95.294
179.56	95.225
189.56	95.162
199.56	95.099
209.56	95.025
219.56	94.947
229.56	94.857
239.56	94.757
249.56	94.646
259.56	94.519
269.56	94.378
279.56	94.224
289.56	94.058
299.56	93.888
309.56	93.726
319.56	93.569

Temperature (°C)	Weight % (%)
329.56	93.408
339.56	93.248
349.56	93.083
359.56	92.92
369.56	92.763
379.56	92.605
389.56	92.443
399.56	92.271
409.56	92.08
419.56	91.872
429.56	91.641
439.56	91.389
449.56	91.114
459.56	90.821
469.56	90.507
479.56	90.166
489.56	89.799
499.56	89.394
509.56	88.979
519.56	88.587
529.56	88.25
539.56	87.975
549.56	87.76
559.56	87.569
569.56	87.396
579.56	87.231
589.56	87.07
599.56	86.912
609.56	86.753

Temperature (°C)	Weight % (%)
619.56	86.606
629.56	86.467
639.56	86.341
649.56	86.223
659.56	86.113
669.56	86.014
679.56	85.931
689.56	85.866
699.56	85.813
709.56	85.754
719.56	85.715
729.56	85.697
739.56	85.671
749.56	85.653
759.56	85.632
769.56	85.609
779.56	85.597
789.56	85.601
799.56	85.578
809.56	85.584
819.56	85.588
829.56	85.591
839.56	85.596
849.56	85.607
859.56	85.622
869.56	85.641
879.56	85.663
889.56	85.702

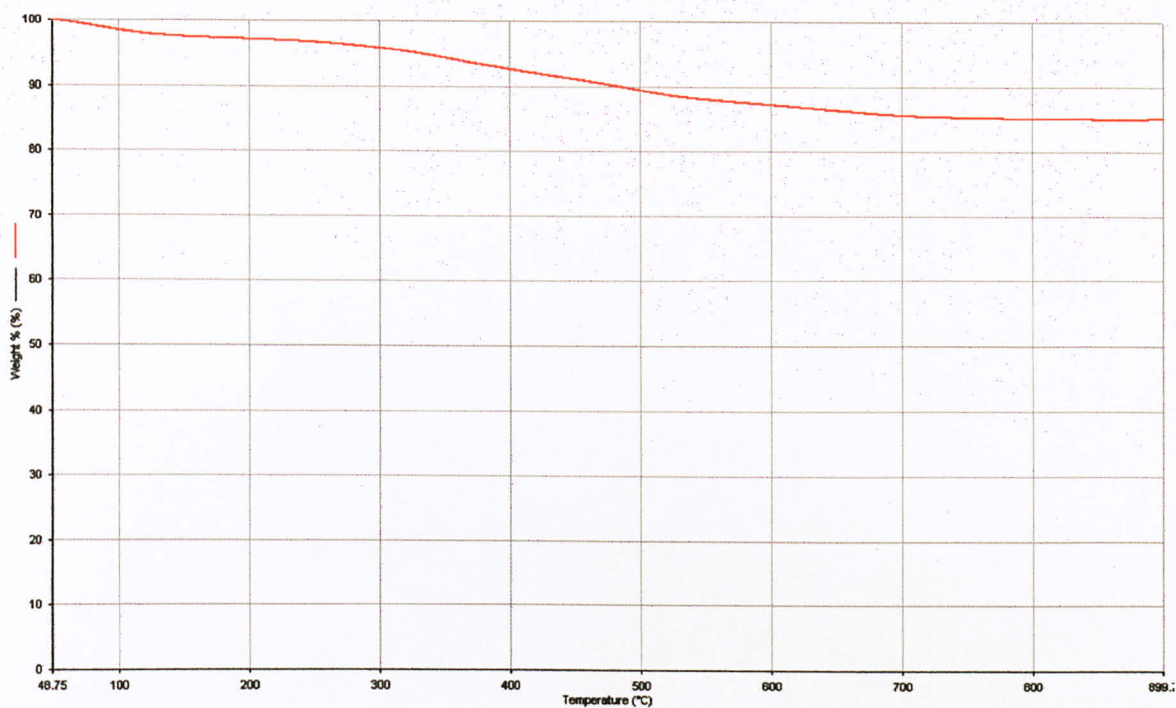


Figure 40: Graph of Weight Percentage (%) vs. Temperature (°C) for EA-Intercalated Ca-Bentonite

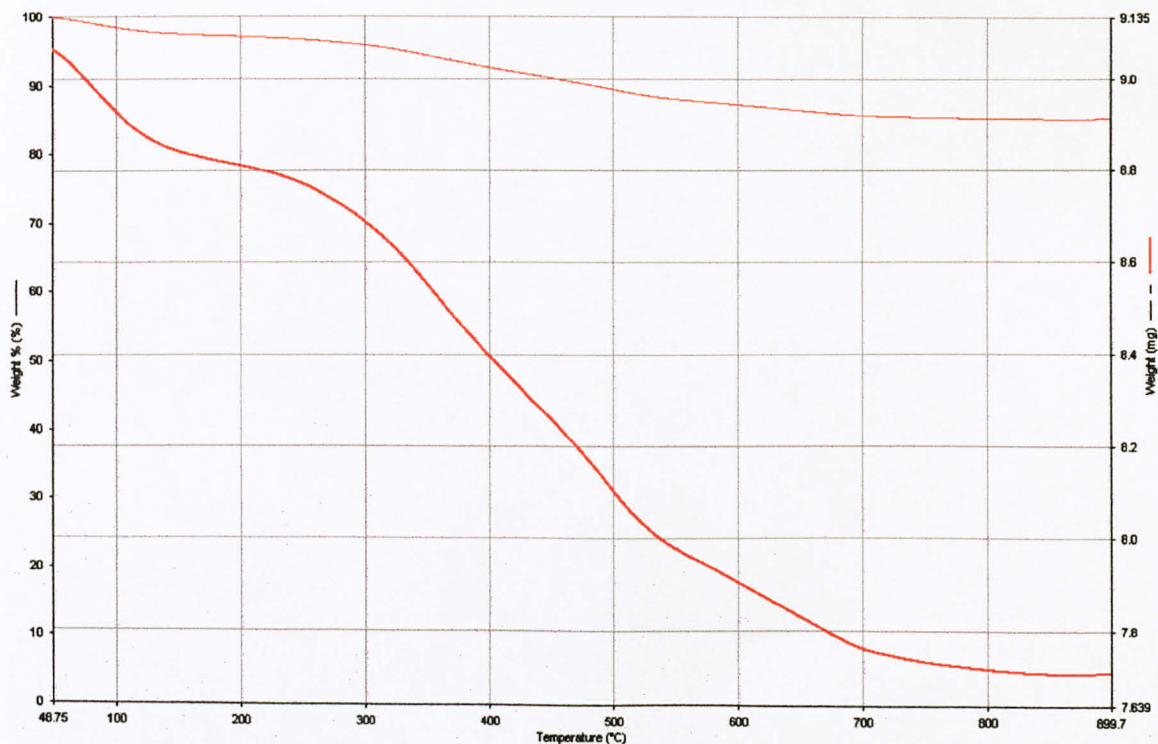


Figure 41: Graph of Weight (mg) vs. Temperature (°C) for EA-Intercalated Ca-Bentonite

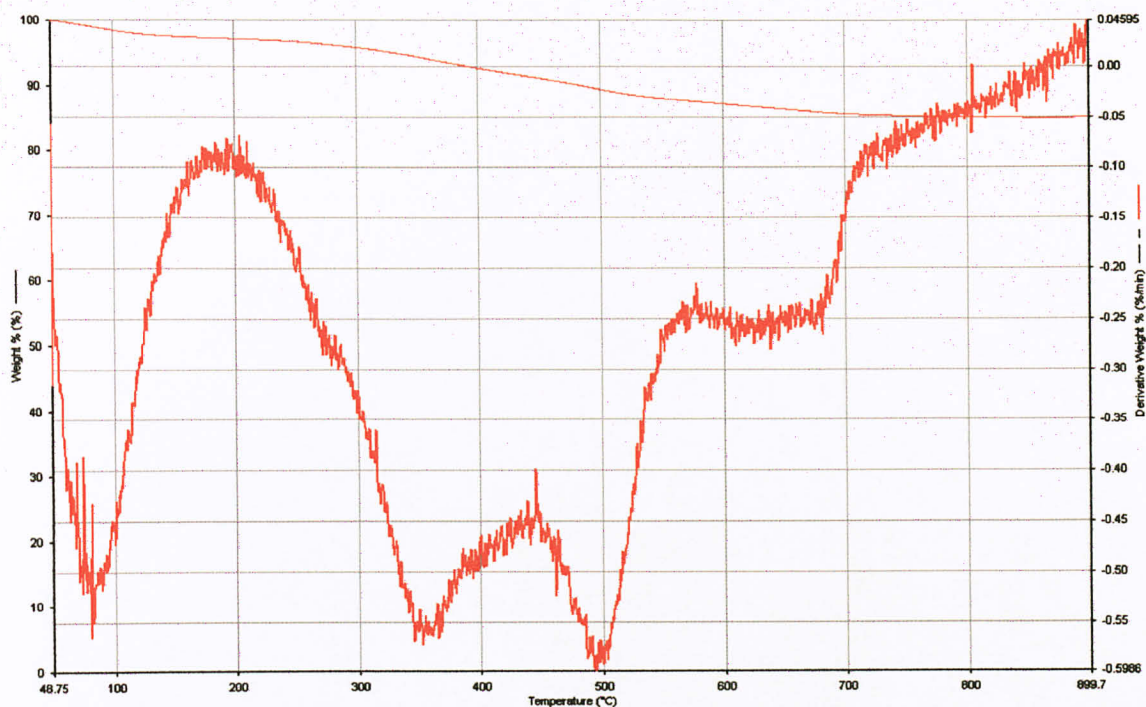


Figure 42: Graph of Derivative Weight (%/min) vs. Temperature (°C) for EA-Intercalated Ca-Bentonite

From these graphs, it can be seen that at about $T=100^{\circ}\text{C}$, there's weight loss attributed to the desorption of physically adsorbed natural water. At $T=400^{\circ}\text{C}$ and $T=500^{\circ}\text{C}$, there is also some weight loss observed, and this is attributed to the desorption of structural water due to the dehydroxillation of the layered aluminosilicate.

Table 7 below shows the weight loss of DEA-Intercalated Ca-Bentonite sample as the temperature is increased $15^{\circ}\text{C}/\text{min}$ in increment of 10°C in the range of $50\text{--}900^{\circ}\text{C}$.

Table 7: Table of Percentage Weight Loss for DEA-Intercalated Ca-Bentonite

Temperature (°C)	Weight % (%)
49.6	99.962
59.6	99.841
69.6	99.709
79.6	99.544
89.6	99.368
99.6	99.188
109.6	98.993
119.6	98.78
129.6	98.538
139.6	98.246
149.6	97.871
159.6	97.411
169.6	96.845
179.6	96.17
189.6	95.394
199.6	94.649
209.6	93.984
219.6	93.439
229.6	92.947
239.6	92.48
249.6	92.02
259.6	91.565
269.6	91.105
279.6	90.65
289.6	90.213
299.6	89.78
309.6	89.36
319.6	88.954
329.6	88.539
339.6	88.125
349.6	87.689
359.6	87.24
369.6	86.791
379.6	86.344
389.6	85.904
399.6	85.49
409.6	85.093
419.6	84.725
429.6	84.368
439.6	84.017
449.6	83.667
459.6	83.312
469.6	82.939

Temperature (°C)	Weight % (%)
489.6	82.156
499.6	81.74
509.6	81.333
519.6	80.918
529.6	80.547
539.6	80.229
549.6	79.953
559.6	79.719
569.6	79.514
579.6	79.336
589.6	79.167
599.6	79.01
609.6	78.861
619.6	78.712
629.6	78.562
639.6	78.409
649.6	78.252
659.6	78.089
669.6	77.915
679.6	77.726
689.6	77.526
699.6	77.324
709.6	77.126
719.6	76.941
729.6	76.781
739.6	76.645
749.6	76.525
759.6	76.427
769.6	76.345
779.6	76.278
789.6	76.219
799.6	76.166
809.6	76.112
819.6	76.061
829.6	76.009
839.6	75.961
849.6	75.914
859.6	75.867
869.6	75.824
879.6	75.784
889.6	75.754
899.6	75.735

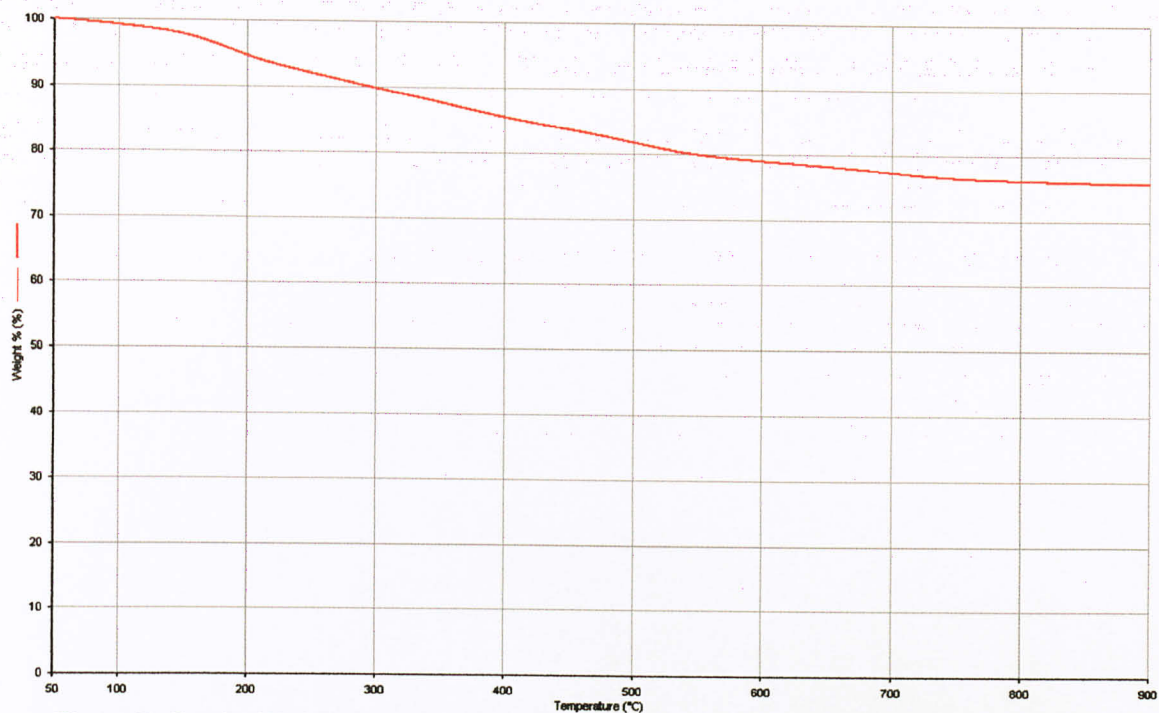


Figure 43: Graph of Weight Percentage (%) vs. Temperature (°C) for DEA-Intercalated Ca-Bentonite

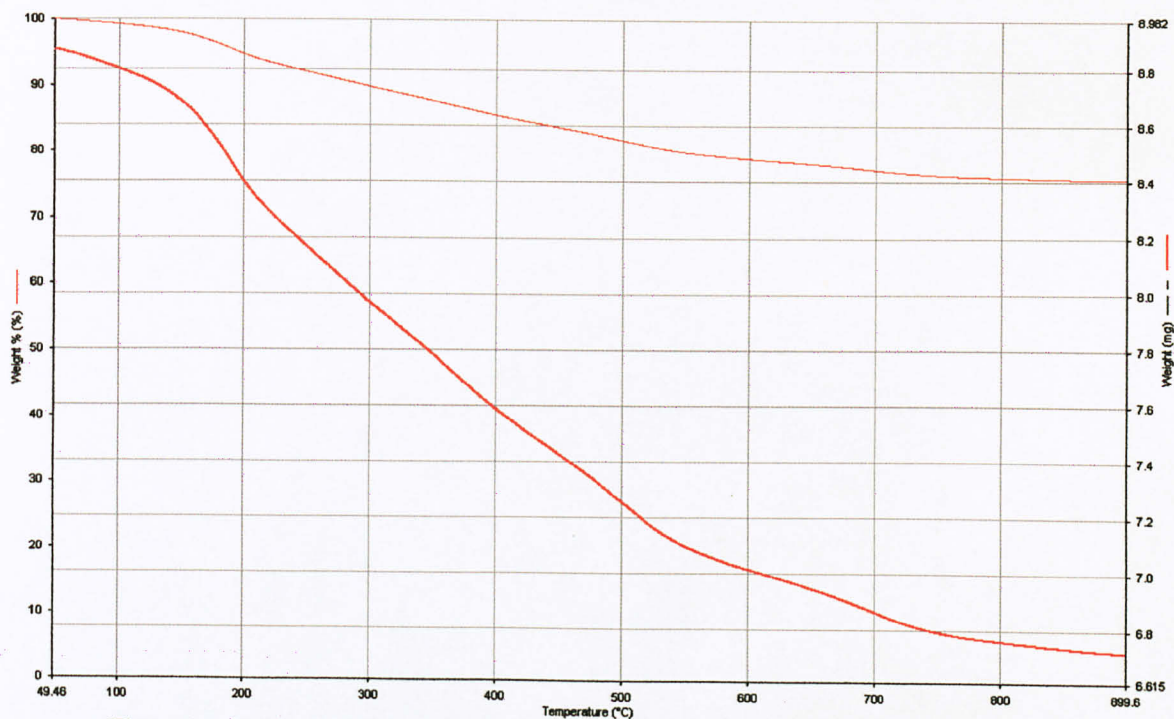


Figure 44: Graph of Weight (mg) vs. Temperature (°C) for DEA-Intercalated Ca-Bentonite

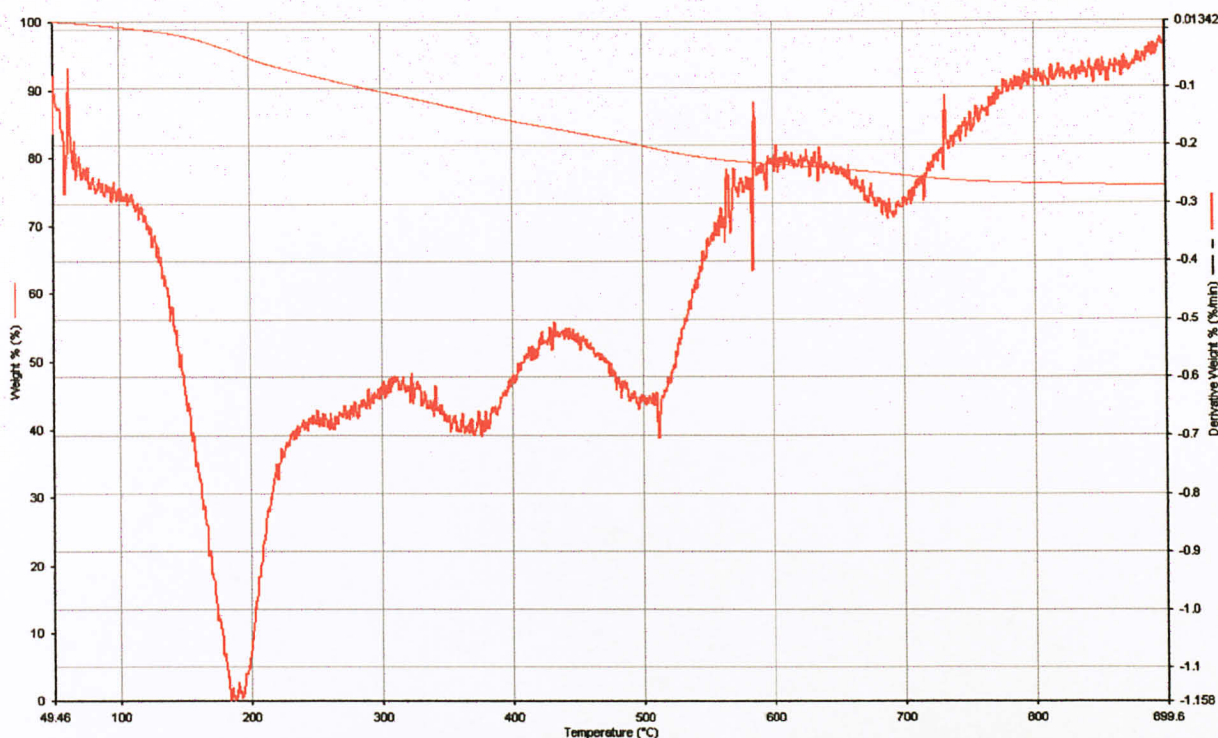


Figure 45: Graph of Derivative Weight (%/min) vs. Temperature (°C) for DEA-Intercalated Ca-Bentonite

From these graph, we can see that at $T=200^{\circ}\text{C}$, there's weight loss attributed to the desorption of physically adsorbed natural water. At $T=500^{\circ}\text{C}$, there is also some weight loss observed, and this is attributed to the desorption of structural water due to the dehydroxillation of the layered aluminosilicate. Also, it is observed that there's further decrease in weight at approximately $T=400^{\circ}\text{C}$ which indicates the amine's loss in weight.

Table 8 shows the weight loss of TEA-Intercalated Ca-Bentonite sample as the temperature is increased $15^{\circ}\text{C}/\text{min}$ in increment of 10°C in the range of $50\text{-}900^{\circ}\text{C}$.

Table 8: Table of Percentage Weight Loss for TEA-Intercalated Na-Bentonite

Temperature (°C)	Weight % (%)
49.4	99.995
59.4	99.995
69.4	99.939
79.4	99.888
89.4	99.843
99.4	99.789
109.4	99.735
119.4	99.68
129.4	99.624
139.4	99.569
149.4	99.508
159.4	99.443
169.4	99.372
179.4	99.294
189.4	99.2
199.4	99.084
209.4	98.962
219.4	98.785
229.4	98.551
239.4	98.27
249.4	97.9
259.4	97.442
269.4	96.944
279.4	96.425
289.4	95.911
299.4	95.357
309.4	94.799
319.4	94.216

Temperature (°C)	Weight % (%)
339.4	92.989
349.4	92.375
359.4	91.714
369.4	91.138
379.4	90.528
389.4	89.884
399.4	89.28
409.4	88.695
419.4	88.128
429.4	87.585
439.4	87.06
449.4	86.546
459.4	86.056
469.4	85.551
479.4	85.04
489.4	84.523
499.4	84.037
509.4	83.58
519.4	83.182
529.4	82.855
539.4	82.585
549.4	82.368
559.4	82.188
569.4	82.033
579.4	81.896
589.4	81.773
599.4	81.655
609.4	81.545

Temperature (°C)	Weight % (%)
619.4	81.434
629.4	81.332
639.4	81.223
649.4	81.12
659.4	81.03
669.4	80.947
679.4	80.871
689.4	80.812
699.4	80.749
709.4	80.694
719.4	80.642
729.4	80.591
739.4	80.541
749.4	80.505
759.4	80.461
769.4	80.447
779.4	80.419
789.4	80.393
799.4	80.354
809.4	80.329
819.4	80.308
829.4	80.293
839.4	80.277
849.4	80.26
859.4	80.246
869.4	80.237
879.4	80.229
889.4	80.231

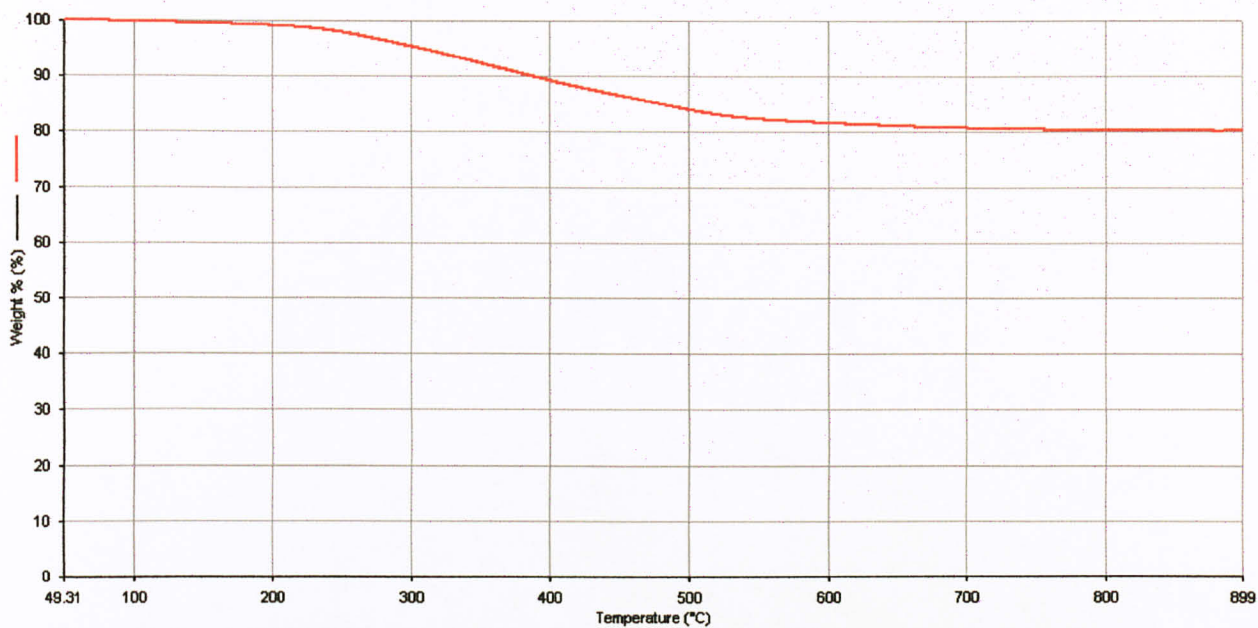


Figure 46: Graph of Weight Percentage (%) vs. Temperature (°C) for TEA-Intercalated Ca-Bentonite

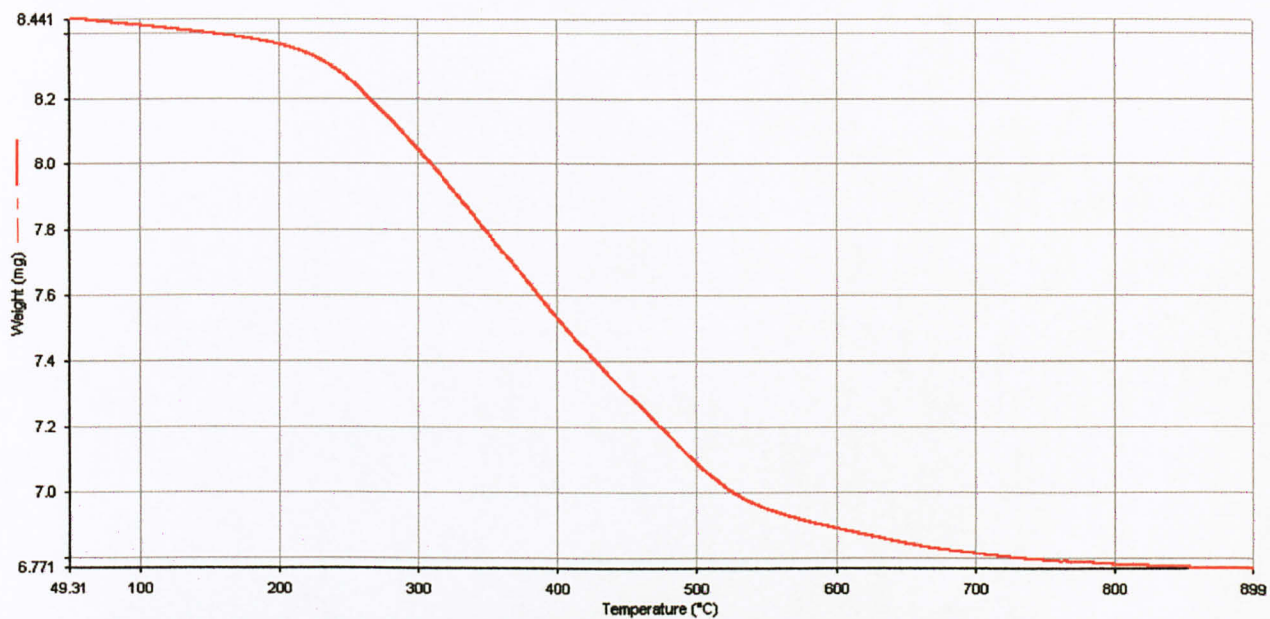


Figure 47: Graph of Weight (mg) vs. Temperature (°C) for TEA-Intercalated Ca-Bentonite

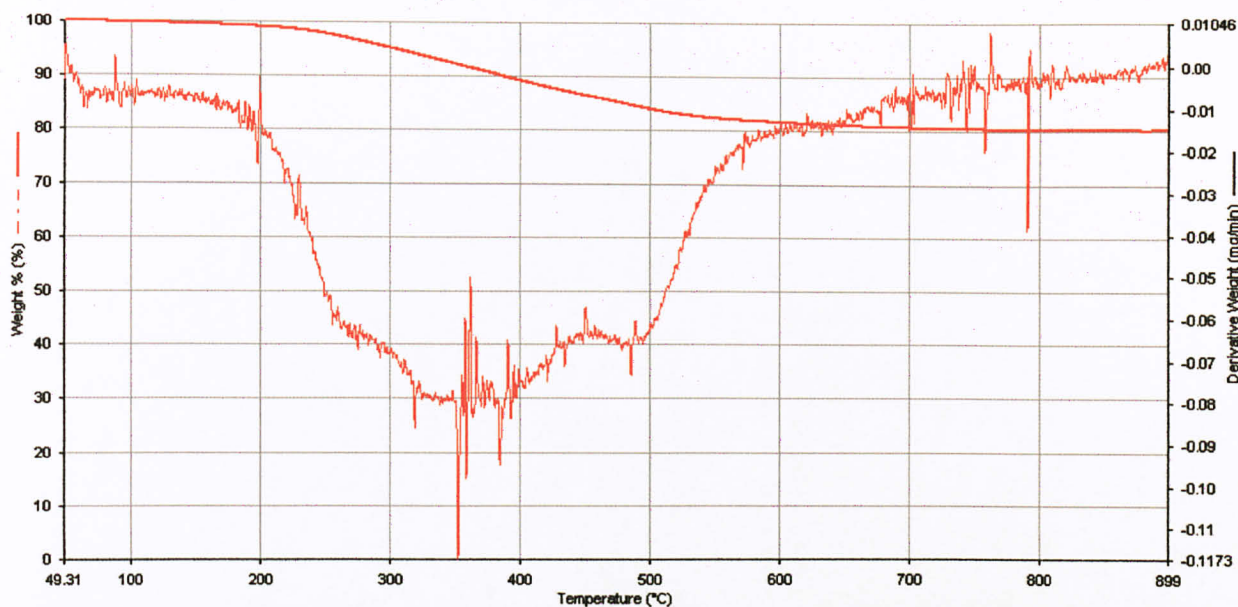


Figure 48: Graph of Derivative Weight (%/min) vs. Temperature (°C) for TEA-Intercalated Na-Bentonite

From these graph, we can see that at $T=100^{\circ}\text{C}$, there's weight loss attributed to the desorption of physically adsorbed natural water. At $T=500^{\circ}\text{C}$, there is also some weight loss observed, and this is attributed to the desorption of structural water due to the dehydroxillation of the layered aluminosilicate. Also, it is observed that there's further decrease in weight at about $T=355^{\circ}\text{C}$ and at approximately $T=780^{\circ}\text{C}$ which indicates the amine's loss in weight.

CHAPTER 5

CONCLUSION

5.1 Conclusion

As a conclusion, it can be stated that the bentonite clay material which is being studied, can be intercalated with possible solvents such as amines and is further possible to develop material to be such as absorbent for CO₂ and heavy metal removal. The final product of this project is bentonite clay intercalated and surface treated with 3 types of amines which are EA, DEA and MDEA.

The first part of the methodology, which is to prepare the intercalated clays, is successfully completed since we now have the final product which had undergone characterization processed such as FTIR, SEM and XRD. Besides that, we also sent the samples for Thermogravimetric Analysis (TGA) and all the results have been discussed.

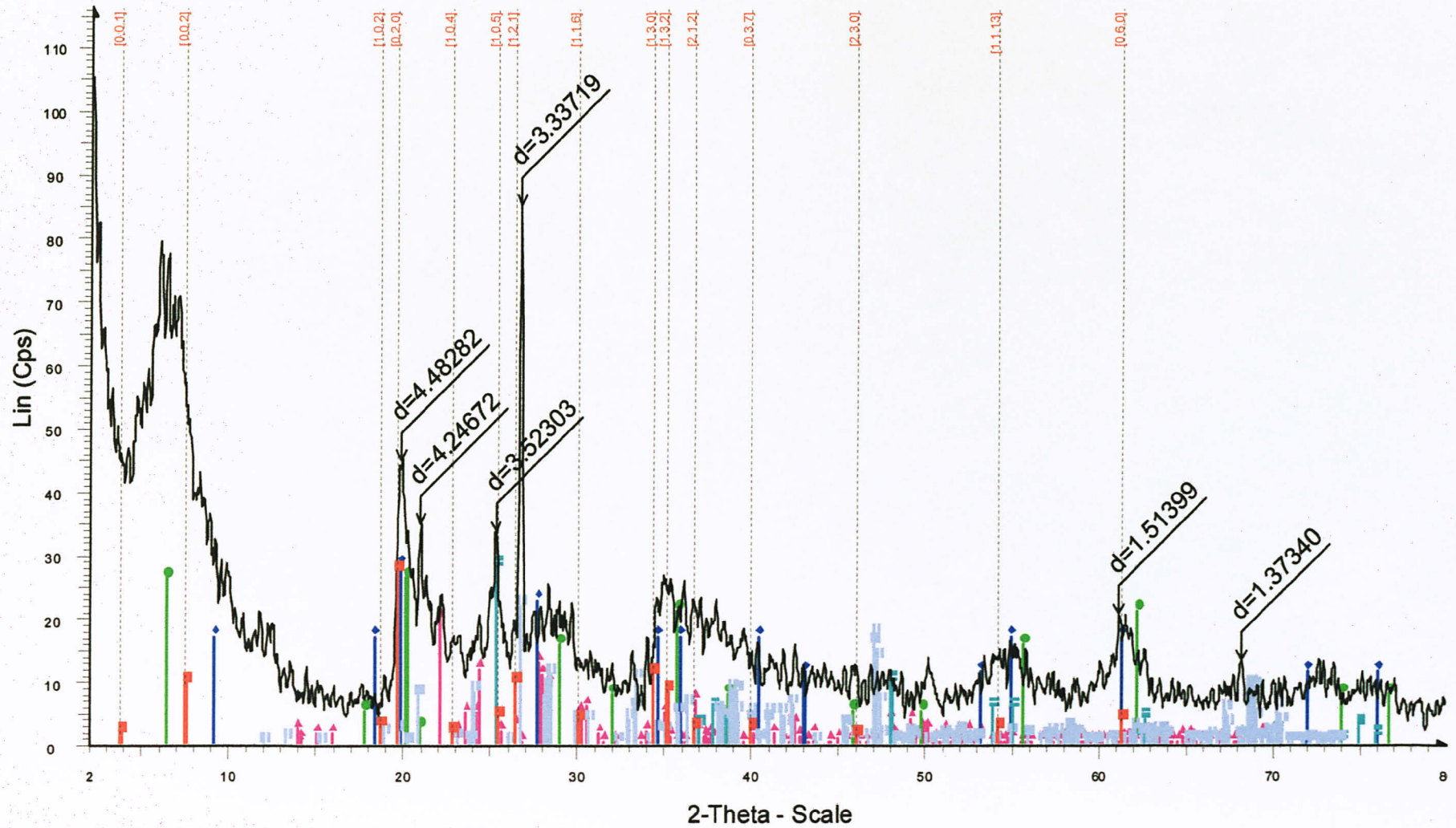
REFERENCES

1. H.H Murray, 2007, "Applied Clay Mineralogy" *Occurences, Processing and Applications of Kaolins, Bentonites, Palygorskite-Sepiolite, and Common Clays*: - 1st Edition, Elsevier Publications, The Netherlands.
2. B. Velde, 1995, "*Origins and Mineralogy of Clays*", Springer-Verlag Berlin Heidelberg, New York.
3. M. Boufatit, H. Ait-Amar, W.R.Mc Whinnie, January 2007, Development of an Algerian material montmorillonite clay- Intercalation with selective long chain alkylammonium cations (Octadecyltrimethylammonium, Cetylpyridium and Tetrabutylammonium) and with tellurium complexes, *Chemical Engineering and Applied Chemistry*, Aston University, Aston Triangle, Birmingham, UK
4. McCabe, Smith & Harriott, "Unit Operations of Chemical Engineering", McGraw Hill, (Singapore), 2001.
5. Robert E. Treybal, "Mass Transfer Operations", Third Edition, McGraw Hill Book Co. (Singapore), 1980.
6. Geankoplis C.J., "Transport Processes and Unit Operations", Prentice Hall, (Singapore), 1995.
7. James R. Connolly, for EPS400-002, Introduction to X-Ray Powder Diffraction, Spring 2007
8. Egerton, R. F. (2005) Physical principles of electron microscopy: an introduction to TEM, SEM, and AEM. Springer
9. Thermo Nicolet Corporation, Introduction to FT-IR, 2001

APPENDIX

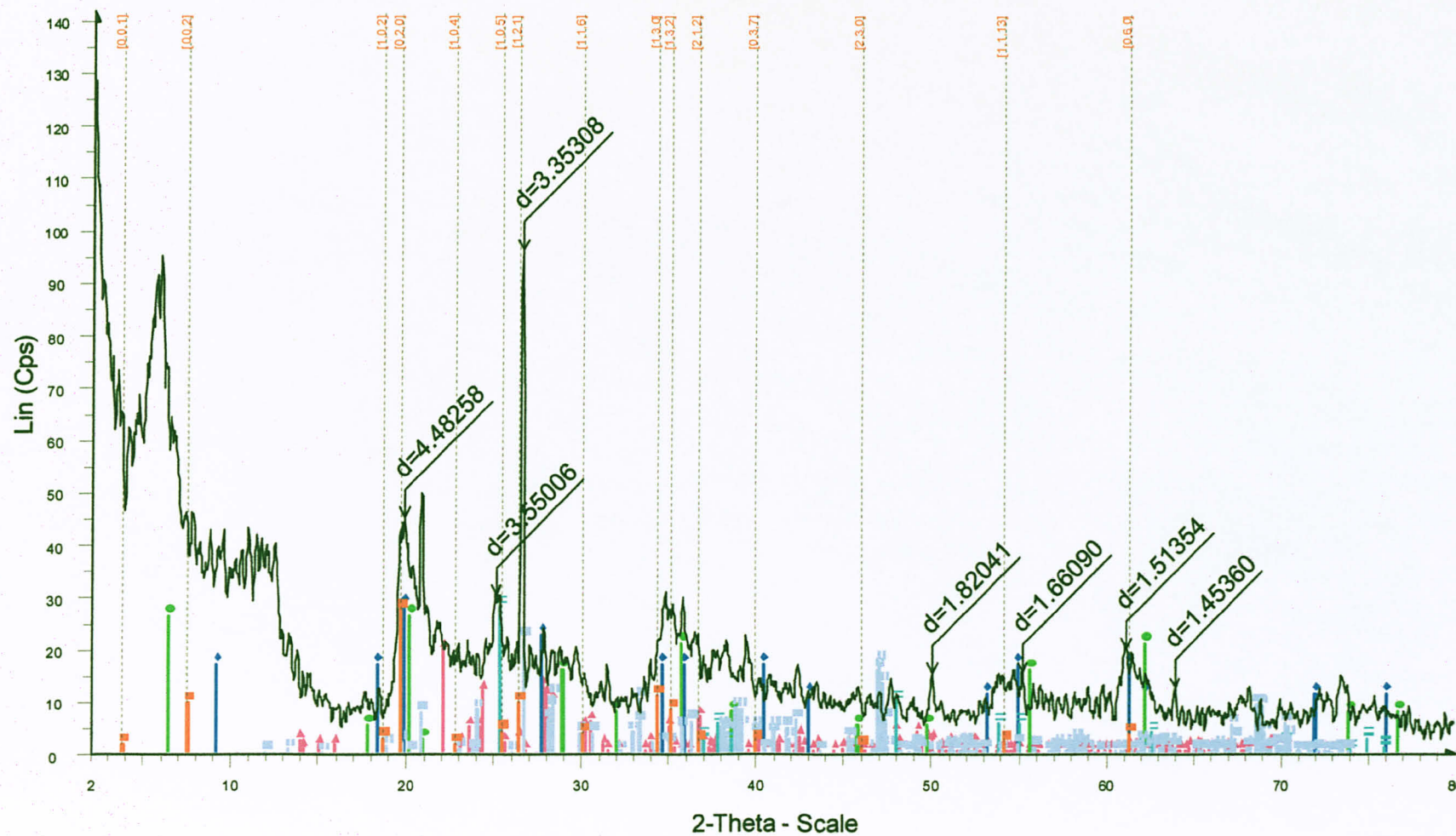
XRD Image for Pure Bentonite

1



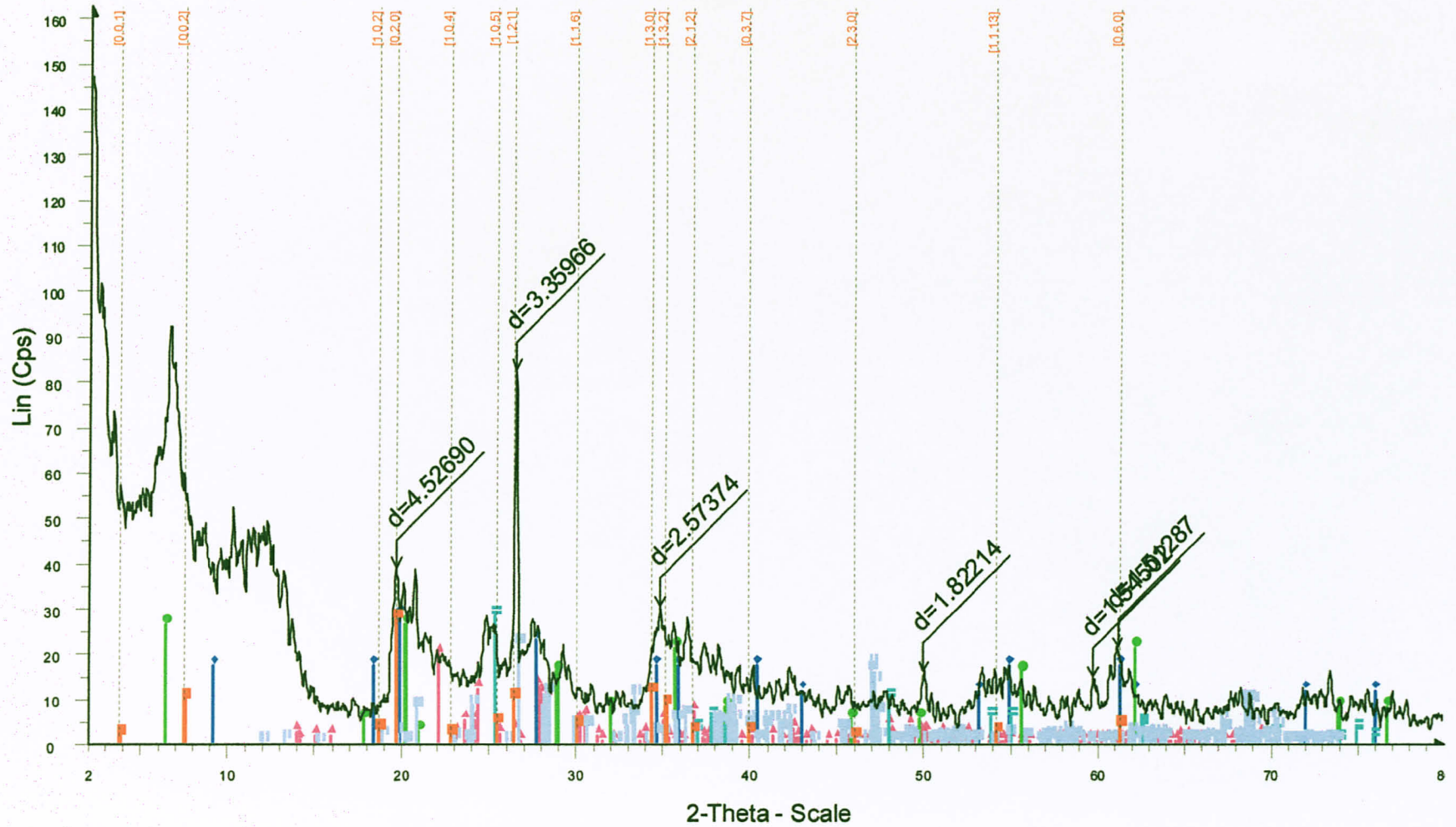
XRD Image for Ca- Bentonite

3



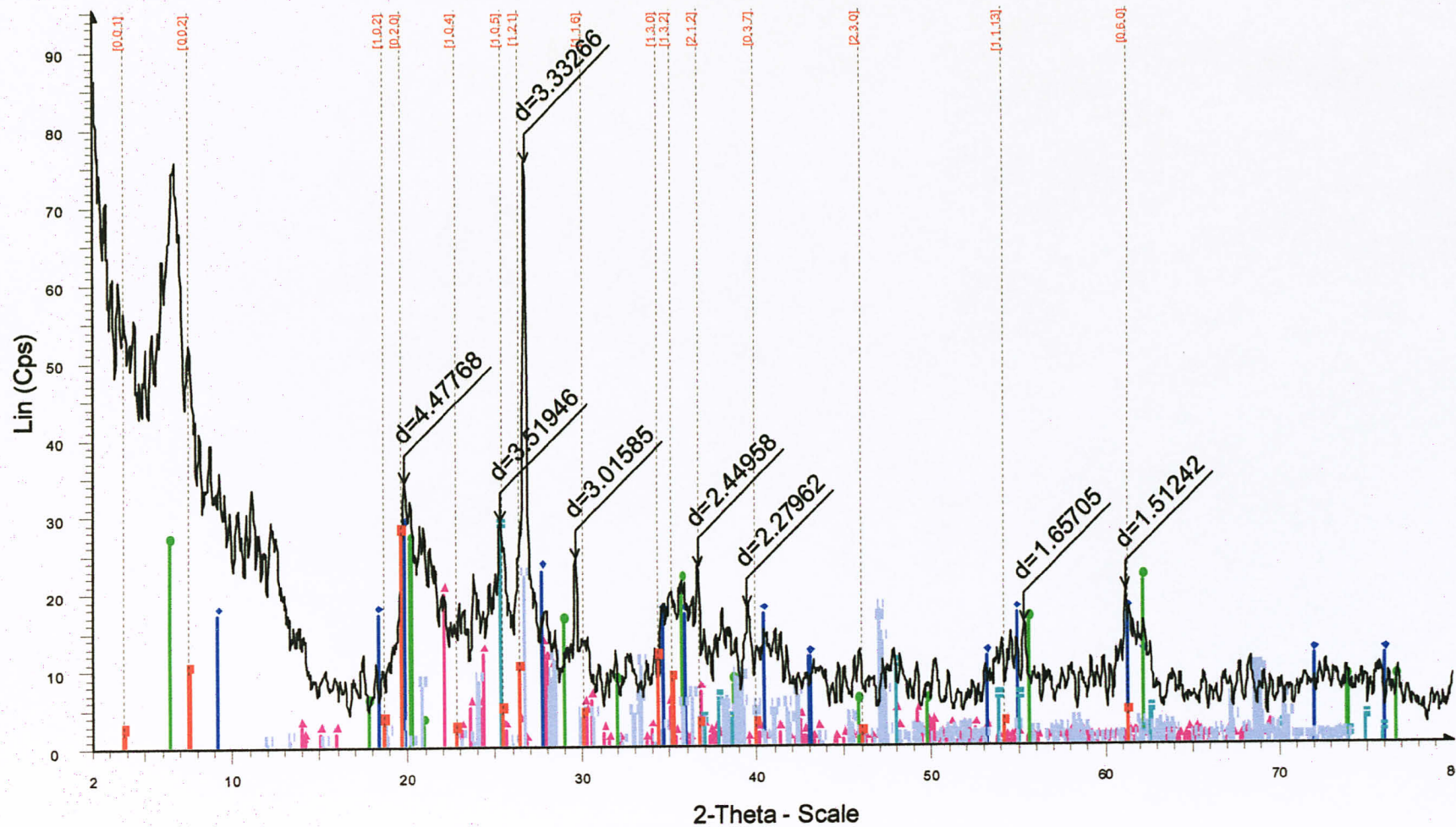
XRD Image for EA-Ca- Bentonite

8



XRD Image for DEA-Ca- Bentonite

7



XRD Image for TEA-Ca- Bentonite

9

